POLITECNICO DI TORINO

Master's Degree in Nanotechnologies for ICTs

Master's Degree Thesis

Enhanced electrochemical sensor sensitivity by using molecular imprinting techniques for the detection of dopamine

Supervisors

Prof. Carlo RICCIARDI

Prof. Tomi LAURILA

Candidate

Giorgia RINALDI

July 2022

Abstract

This study investigates a molecularly imprinted electrochemical sensor for sensitive dopamine (DA) determination. The purpose of this work is to develop high-performance and miniaturizable sensors for DA, a neurotransmitter (NT) involved in many neurological diseases. The concentration of NTs in the human body is extremely low and, for this reason, the sensor utilized for their detection should have physiologically relevant sensitivity.

Molecular imprinting consists of the formation of a polymeric layer modified with recognition sites to a particular target analyte. This is carried out through the polymerization of the functional monomer in the presence of the target. The electrodes developed in this study are based on a silicon substrate, modified with a tetraheadral amorphous carbon (ta-C) layer and a DA imprinted polypyrrole (PPy) layer. The molecular imprinting of pyrrole was carried out electrochemically through cyclic voltammetry (CV) in the presence of DA. The ta-C layer has been involved in order to further improve the performance of the electrode, as it provides extremely interesting properties.

The proposed MIP-based sensors have been studied electrochemically by CV, differential pulse voltammetry (DPV) and electrochemical impedance spectroscopy (EIS) and they showed an enhanced performance with respect to their non-imprinted counterpart. The limit of detection (LOD) was measured to be in the nanomolar range ($48.6\,nM$), which ensures a physiologically relevant sensitivity ($162\,nM$).

First the experimental conditions were optimized in order to improve the performance of the electrodes. Electrochemical and physical (SEM, AFM, Raman spectroscopy) characterizations were carried out in order to better understand the behaviour of the sample in the sensing system. The performance of the designed MIP/ta-C electrodes towards DA was studied at different DA concentrations and in the presence of interferents. Finally the effect of the thickness of the ta-C layer and of the presence of a titanium adhesion layer were considered.

The current work has been carried out at the Department of Electrical Engineering and Automation at Aalto University. In particular, the facilities in which the studies have mainly taken place are at Micronova, Finland's national research infrastructure for micro- and nanotechnology.

Acknowledgements

I would like to thank professor Tomi Laurila and his research group at Aalto University for hosting me and for teaching me everything I know about electrochemistry in the last six months. A special thanks goes to Rahil for her precious teachings and her continuous support.

I wish to show my appreciation to professor Carlo Ricciardi for guiding me during my thesis semester and my path abroad.

Last but not least, a heartfelt thanks to my family, for their continuous support and advise during my path. Thank you for your deep trust in me and for your love.

Table of Contents

Introduction

One of the most interesting challenges of our times is the monitoring of the state of the human body and its functions by means of sensors. Electrochemical sensors rely on the performance of an electrode in direct contact with the biological environment and, for this reason, it is important to design them carefully [1].

Neurotransmitters (NTs) play a fundamental role in the regulation of brain functions and, as a result, any imbalance in their activity can bring about neurological diseases such as Parkinson's, schizophrenia and Alzheimer's. The diagnosis, monitoring and treatment of such mental illnesses is therefore relying on high performance sensors, which are expected to monitor NTs concentration and activity [2, 3]. The burden of neurological diseases in Europe has been studied and it has been found that, in the EU, neurological disorders are the third cause of total DALYs (disability-adjusted life-years) [4]. Furthemore, the neurological disorders are meant to increase, as the amount of elderly people in the population is increasing rapidly [5]. Neurological diseases are often related to changes in spacial and temporal kinetics of NTs, as the brain functioning is strictly related to their controlled dynamics. As a consequence, the accurate sensing of NTs is an important tool to better understand the current treatments and develop new ones [5]. Focusing on the detection of dopamine (DA), it is of vital importance to accurately determine its levels *in situ* for therapeutic purposes, but also to improve the knowledge in neural pathophysiology, moving towards new therapeutics and diagnostic tools [6]. Unfortunately, NTs levels are extremely low in the extracellular fluid and, for this reason, sensing systems are required to be extremely sensitive. Furthermore, as a high number of interferents is present, sensors must be highly selective as well. These interferents often have similar oxidation/reduction potentials to the target, which makes the detection extremely challenging. Finally, DA is rapidly released and cleared from its medium after its release and, as a consequence, fast response time is vital. Long term stability is another desirable property for a DA sensor, as electrode fouling is one of the biggest challenges [1, 2].

Electrochemical sensors are a valuable tool for the detection of NTs, thanks to their low cost, short time required for the analysis and multi-analyte detection.

Furthermore, they are suitable for *in situ* detection and could be exploited in point-of-care (POC) testing devices [3]. Focusing on in vivo measurements, the most important challenges are: (i) multi-analyte detection maintaining high temporal resolution in real time, (ii) long-term monitoring. The ultimate goal is to develop a sensing system that could monitor in real time the dynamic behaviour of different NTs in order to monitor and treat patients affected by neurological disorders. It would be also interesting in the future to be able to detect multiple NTs at the same time *in vivo*, as most disorders are caused by the rupture of the equilibrium between several ones [2]. One of the goals for the future is the development of implantable (bio)sensors for continuous monitoring of human health states and disease development, together with the simultaneous detection of multiple NTs through electrode arrays and real time, continuous monitoring [3]. A challenge along this work will be to obtain *in situ* monitoring of DA with high specificity and high temporal and spacial resolution [7]. It is therefore expected that the future of (bio)sensing will be focused on the development of array biosensors, biochips and POC devices for multiple analyte studies. This way, all processing steps will be integrated into a micro-analytical system, reducing the time needed for the results and the volume of reagents [8].

The present work aims at the description of a research project based on the development of a molecularly imprinted electrochemical tetrahedral amorphous carbon (ta-C) based sensor for high sensitivity detection of DA. The surface of the silicon substrate of which the electrode is made of is further modified in order to build up the sensing system. This has been carried out by coating the silicon substrate with a ta-C bidimensional layer and with a conductive polymer (PPy) based molecularly imprinted polymer (MIP) layer. Table 1 summarizes the reason why the elements of surface modification were chosen for the sensing system under analysis.

The description of the work investigates first the theoretical background under the sensors development, describing more in depth the following topics:

- What are NTs (section 1.1)
- NTs detection methods (section 1.2)
- Conducting polymers (section 1.3)
- Molecular imprinting technology (section 1.4)
- Surface modification with carbon nanomaterials (section 1.5)
- State of the art (section 1.6)

After that, the objective of the work has been better discussed, going into the details of the experimental work (chapter 2). The experiments have been then

described, focusing on the materials and methods used for the various studies (chapter 3). Finally, the results are presented and discussed (chapter 4).

Features of the developed sensors	**Reasons**
MIPs	High selectivity High resistance to environmental factors Prevents passivation of the electrode
Carbon nanomaterials, ta-C modification	High sensitivity High conductivity Wide voltage range Fast electron transfer
Conducting polymers, PPy	Biocompatible Improved sensitivity Imprinting at room temperature Easy template removal and rebinding

Table 1: Reasons the different building blocks of the electrodes under investigation were selected

Chapter 1

Theoretical background

1.1 Neurotransmitters: focus on dopamine

The neuron is the fundamental unit of the nervous systems. It is made of a nucleus, the *perikaryon*, axon and dendrite, as shown in figure 1.1. The nucleus is connected to one longer protrusion called axon and several shorter ones called dendrites: the latter ones provide the input to the neuron, while the axon (with many branches) is sending outputs outside. The neurons are connected to one another through synapses, which are the junctions connecting the terminal of an axon of one neuron (called pre-synaptic neuron) to the dendrite of another neuron (called post-synaptic neuron). Dendrites are the input elements of the neuron and they branch off from the nucleus. They are needed for the reception of signals through specialized receptors: they play a fundamental role in the filtering and integration of synaptic inputs to decide whether to fire or not. Axons are instead the output element of the neuron and they are useful for long distance transmission from the neuron to the axon terminal. The synapse is another very important region of the neuron, as it is the structure used for the transmission of the signal between the pre-synaptic axon and the post-synaptic dendrite. Synapses can be either electrical or chemical. Electrical synapses pass ionic currents to induce voltage changes directly in the post-synaptic cell, while chemical synapses electrical activity is converted into chemicals for the transmission [9, 10].
In any case, in order to transfer information between neurons, an electrical signal is employed: this is called action potential. This is able to travel through neurons and it can enable the release of chemicals, called *NTs*, in chemical synapses across the synaptic cleft, as shown in figure 1.1. The synaptic cleft, in particular, is the gap between the synapses and, more precisely, it stands between the pre-synaptic axons and the post-synaptic dendrite; it is the center of the communication between neurons. Therefore, in chemical synapses, the electrical signal coming from the

dendrite is converted into chemical with the release of NTs and then again into the electrical signal propating through the axon. For this reason, NTs are considered to be the chemical messengers of the body: they are used by the nervous system to transmit information between neurons or from neurons to muscles [9, 10, 11].
The action potentials are able to open the vescicles containing the neurotransmitter molecules. At this point, the signal becomes a chemical one, and a specific response is caused in the receiving neuron, which accepts the neurotransmitter molecules thanks to receptors. In particular, the neurotransmitter released is able to excite or inhibit the second neuron from firing its own action potential. As a consequence, the signal goes back to being electrical. In particular, depending on the direction of the current in the synapse, the membrane potential can be increased or decreased, modulating the connection between the two neurons. This modulation is termed *synaptic plasticity* and it refers to the ability of neuron and synapses to change their properties and, in particular, the synaptic strength [10, 11].
The human nervous systems is a mesh of neural networks organized in a hierarchical way to provide several computational functions such as vision, audition and emotion. This hierarchy determines the top level of organization of the brain. The medium level is described by neurons, which can be considered to be the basic unit of this level of organization [10].
The role of a neurotransmitter can either be excitatory, inhibitory or mudulatory. Excitatory NTs promotote the generation of an action potential in the receiving neuron, while inhibitory NTs are able to prevent it. Differently, neuromodulators are able to affect a larger number of neurons and they are not restricted to the synaptic cleft [11]. Some examples of excitatory NTs are acetylcholine, epinephrine, norepinephrine, serotonin and glutamate; inhibitory ones include istead γ-aminobutyc acid and glycine. Dopamine (DA) is considered to be a special case, as it shows both inhibitory and excitatory functions [6].

NTs can also be divided into fast, if they operate in the millisecond time domain, or slow, if they work in the second/minute/hour time domains. DA belongs to the slow-acting NT category [9, 11].

Another classification criterion for NTs is according to their chemical nature; they can be divided into the following categories:

- Amino acids (e.g. Glutamate, Tyrosine)
- Biogenic amines (e.g. **DA**, Epinephrine)
- Acetyl cholines (e.g. Acetylcholine)
- Soluble gases (e.g. Nitric oxide, Hydrogen suphide)

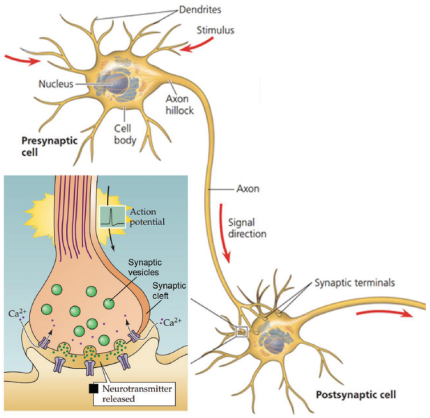

Figure 1.1: Structure and working principle of a neuron [10]

NTs are a very important part of the synaptic transmission process. Any imbalance in their activity is a cause for serious mental disorders, such as psychotic and neurodegenerative diseases like Parkinson's, Alzheimer's and Huntington's diseases, but also physical illnesses. Other neural diseases related to NTs imabalance are stroke, epilepsy, traumatic brain injury (TBI), cerebral meningitis, but also various mental disorders such as depression, anxiety, schizophrenia and bipolar disorder. Many brain functions can be related to NTs, such as behaviour and cognition, cardiovascular, renal and hormonal function systems, as well as the enstablishment of brain-body integration. NTs also regulate sleep, mood, learning, memory, appetite, concentration and other cognitive functions. At last, altered levels of NTs could also represent substance use disorders [3, 6]. It is therefore important to develop high performance sensors for the detection of NTs, in order to understand their biochemical and physiological roles under various stimuli. NTs analysis could lead to essential breakthroughs for the understanding of the functioning of the brain and its disorders, and in turn to better clinical assessment [7, 12].

The chemical working principle of neurons was first understood studying the effect of poisons on animals. As poisons can mimic nerve stimulation, a chemical response has been theorized. Studies started to show that in order to allow the conduction of a signal in the brain, the gap between two neurons has to be crossed. Otto Loewi was the first to discover the emission of chemicals in response to activation, namely an electrical signal. Loewi studied vague nerves in frogs, leading to evidence of the release of chemicals when the nerve was stimulated. In particular, he proved that when the vague nerve to the heart was stimulated, a substance was released into the perfusion fluid and the heart slowed; furthermore, when the perfusion fluid was used for a second heart free of any stimulation, this second

heart also slowed down. This first study was then expanded leading to the naming of the process as *neurochemical transmission*; the chemicals involved in the process were instead called *NTs* [9]. The first NT was discovered by Loewi himself in 1921 and it was acetylcholine. For this research, Loewi has been awarded with the Nobel Prize in 1936, jointly with Sir Henry Dale. After that, many other NTs have been discovered: nowadays more than 100 types are known [2, 13].

DA is a NT synthesized in the kidney and in the brain; it is responsible for reward, mood, motivation, memory and perception-based aspects, as well as motor functions. It belongs to biogenic amines, also called catecholamines, together with epinephrine and norepinephrine: such molecules, like amino acids, are characterized by a nitrogen-containing group and by a lack of carboxyl groups. As shown in figure 1.2, the DA molecule shows a catechol ring and an amine side chain. Biogenic amines, in general, play an essential role in the regulation of central and peripheral nervous systems. In particular, DA is essential in hormonal, cardiovascular, renal and mammalian central nervous systems. In addition, neurological disorders as Alzheimer's and schizophrenia show abnormal levels of DA [3, 6, 14].

Catecholamines, as hormones, can be found in human blood and they can be extrected in human urine. As a result, they can be detected in biological fluids such as human serum and urine and they can be used for dignostic purposes [15].

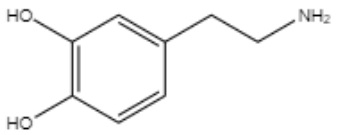

Figure 1.2: DA molecule

The biosynthetic pathway of catecholamine is shown in figure 1.3. The enzyme Tyrosine hydroxylase (TyrH) is rate-limiting for the synthesis of catecholamines. TyrH catalizes the hydroxylation of tyrosine to l-3,4-dihydroxyphenylalanine (L-DOPA) and DA, epinephrine and norepinephrine are products of the pathway. As seen in the figure 1.3, phenylalanine hydroxylase converts phenylalaline to tyrosine; then, the hydroxylation of tyrosine occurs by means of tyrosine hydroxylase reaching L-DOPA. As a consequence, DOPA is then converted into DA thanks to decarboxylase, an aromatic amino acid. The biosynthetic path goes then on with the synthesis of norepinephrine and epinephrine [16].

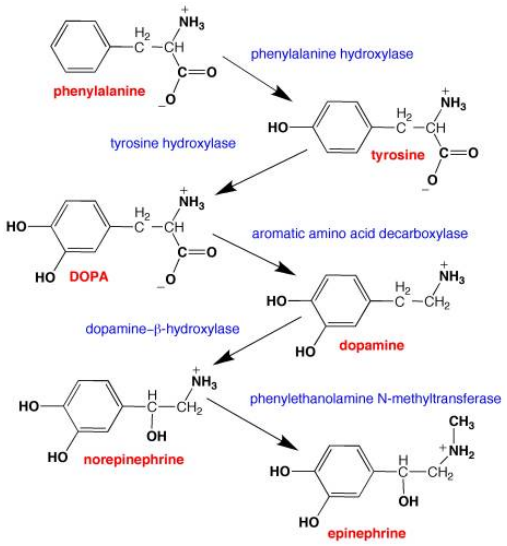

Figure 1.3: Biosynthetic pathway of DA [16]

It is interesting to go through the oxidation pathway of DA, which could be exploited for the electrochemical sensing thereof. Figure 1.4 shows the $2e^-/2H^+$ redox reaction undergone by DA when a potential is applied. This reaction enables the electrochemical detection of DA, which will be studied in further detail in section 1.2. The transfer of two electrons and two protons required in the reaction will bring about the production of DA quinone, the product of DA oxidation. The current generated by the charge transfer is proportional to the concentration of DA, leading to the electrochemical quantification of DA [12].

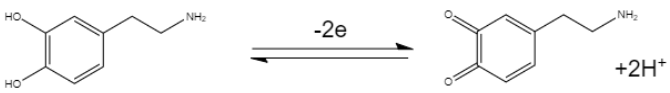

Figure 1.4: Oxidation reaction of DA

DA has several analogues, such as norepinephrine, L-Dopa and epinephrine, but also some potential interferents (uric acid and ascorbic acid). This complicates its detection and requires high specificity in the sensors employed. The reason why these molecules interfere with the detection of DA is their susceptibility to oxidation, just like DA. In conclusion, techniques to ensure the specificity of the sensors need to be employed; some of them can be the use of biological ligands or molecular imprinting [7]. As mentioned above, it is possible to enhance sensitivity and selectivity of the electrodes by means of to DA modifying the electrode with nanomaterials and affinity ligands [7]. The methods discussed in this work are

conducting polymers (CPs) (section 1.3), molecular imprinting (section 1.4) and carbon nanomaterials (section 1.5).

DA concentration in an healthy subject is supposed to be between $0.001\,\mu M$ and $1\,\mu M$. A high DA level could be a sign of cardiotoxicity, leading to high heart rates, hypertension, heart failure and drug addiction. Furthermore, high dopaminergic activity could lead to errors in perception, such as hallucinations and psychiatric diseases (e.g. schizophrenia). In contrast, low dopaminergic activity is generally related to neurological and motor disorders: a low DA level could cause stress, Parkinson's disease, schizophrenia, Alzheimer's disease and depression [7, 12, 14]. It is important to measure the concetration of DA *in vivo* in order to be able to understand the role of DA in neurological functions and diseases [17]. Table 1.1 shows some examples of disorders related to DA lack or abundance.

Condition	**DA concentration**
Parkison's disease	Almost complete depletion - 1.22 ng/mL
Alzheimer's and schizophrenia	1.89-189 ng/mL
Pure anatomic failure and multiple system atrophy	0.007-0.015 ng/mL (in cerebrospinal fluid)

Table 1.1: Examples of conditions related to DA imbalance [18]

1.2 Neurotransmitters detection methods

The detection of NTs can be carried out with several analytical methods; some examples of them are:

- Brain microdialysis [6]
- Mass spectroscopy (MS) [6]
- Fluorescence [3]
- Chromatography (often high pressure liquid chromatography, HPLC) [3, 6]
- Imaging techniques such as electroencephalography (EEG) and magnetic resonance imaging (MRI) [6]

Unfortunately, these techniques are expensive, time consuming and they need highly trained personnel; in addition, they require complex sample preparation methods [3, 6].

Several other transduction mechanism can be used in order to overcome the complexity of the analytical methods, such as optical, piezoeletric, acoustic, gravimetric, magnetic, calorimetric and electrochemical. Among the methods listed above, the two most promising ones are the optical and electrochemical methods [3, 6]. Electrochemical sensors, in particular, are characterized by several attractive qualities listed in table 1.2. Unlike the analytical techniques mentioned above, electrochemical ones can be adapted for the detection of a wide range of analytes; they can as well be incorporated into robust, portable and even miniaturisable devices while keeping the cost low [6, 19].

Advantages of electrochemical detection	**Disadvantages of electrochemical detection**
• Low cost • Good sensitivity • Rapid response • Easy miniaturization • Linear input and low power requirements • Good resolution and accuracy • Excellent repeatability • Simple modification	• Slow commercialization • Narrow optimization range • Analyte and sensing interface based reaction is limited, as the detection is restricted • Variations in electrode materials require calibration in each experiment

Table 1.2: Advantages and disadvantages of electrochemical sensing

Electrochemistry is an appealing technique, as it converts directly the chemical information into an electrical signal with great detectability, simplicity and cost [6, 19].

Electrochemical detection is inexpensive, it does not need much time to deliver the results, and more than one analyte can usually be detected simultaneously. As a result, electrochemical detection of NTs easily outdoes analytical methods [3, 6]. In addition, electrochemical methods depend on surface phenomena, opening to the possibility of using very small sample volumes and of miniaturization. The latter is one of the greatest strength points of electrochemical sensing, as it paves the way to micro and nanotechnologies [6, 19].

Electrochemical sensors are a dynamic field of research, especially when nanoscience and nanotechnolgies come into play. Nanotechnologies could in fact benefit the development of electrochemical sensors in many ways, which are summarized in the following [6, 19]:

- Improved sensitivity
- Quick response time and high throughput
- Low power demand and cost
- Easy device fabrication and recycling
- High surface area and nanoparticles enhance low detection limit
- Higher stability, high surface energy and potential biocompatibility
- Excellent optical and electrical properties of metallic nanoparticles improve sensing capability
- Catalytic properties of nanoparticles and fluorescent property of quantum dots (QDs) ameliorate detection
- Improved portability

Furthermore, the easy miniaturization of electrochemical sensors can be exploited for on-site detection and be, in the future, used as point-of-care testing devices. The development of innovative sensors can be carried out by means of nanotechnologies and improved data analysis, leading to highly performing devices [3, 6, 19].

Electrochemical sensors are also characterized by the advantage of being able to operate in complex biological media [3, 6]. Another advantage of electrochemical sensing is the wide range of applications. They are in fact widespread used in daily life and they make use of rapid, simple and cheap methods for the detection of several analytes [19].

1.2.1 Working principle of electrochemical sensing

Going into the details of electrochemical sensing, it is important to describe its working principle [8]. Chemical sensors are devices able to convert chemical information by means of a chemical reaction in a selective and reversible way. Electrochemical ones are a subset of those and they are based on chemical reactions producing an electrical signal proportional to the concentration of the analyte [8]. They couple a biological recognition element to a solid electrode surface: they respond to the applied electrical impulses and convert the biorecognition process into an electrical signal. Electrochemical sensors, in particular, record the presence of neurotransmitters through oxidation or reduction at solid support [8].

Several properties should be taken into account when developing electrochemical sensors [19]:

- Cost
- Miniaturisation
- Sensitivity
- Sensor reproducibility
- Selectivity and specificity
- Multi-analyte detection
- Stability

Among these, the most challenging parameter is the low sensitivity of electrochemical sensors. It can be improved by controlling electron transfer kinetics and diffusivity of electroactive species [8]. The immobilization of the probes, when needed, is another parameter affecting sensitivity, as it can lead to a loss of binding capacity [8]. As mentioned above, nanotechnology is a powerful tool to improve the sensitivity of electrochemical biosensors, as nanomaterials have excellent electronic properties, electrocatalytic activity, high surface area and more, as presented in section 1.5 [8]. Selectivity can be considered to be another challenging property, especially for *in vivo* measurements and a trade-off between it and other parameters is often required [19]. A solution for enhancing the selectivity of the electrochemical sensor is the use of MIPs [18, 15], which have been dealt with in section 1.4.

Going deeper into electrochemistry, it is worth mentioning that controlled-potential analytical experiments have the goal of returning a current response proportional to the concentration of the target analyte [20]. This is accomplished by monitoring the redox reaction undergone by the target analyte, which can be generally described as:

$$O + ne^- \rightleftharpoons R \tag{1.1}$$

In the previous equation, the O represents the oxidized species and the R the reduced one; they form the redox couple [20]. A useful tool for the quantification of electroactive species at the surface of the electrode is the Nernst equation:

$$E = E^0 + \frac{2.3RT}{nF} log \frac{C_0(0,t)}{C_R(0,t)} \tag{1.2}$$

where E^0 is the standard potential for the redox reaction, R is the universal gas constant ($8.314\ K^{-1}mol^{-1}$), T is the temperature in Kelvin, n is the number of electrons transferred in the reaction and F is the Faraday constant ($96.487\ C$) [20]. The change in the oxidation state of the electroactive species will generate a current, which is generally called *faradaic current* as it obeys Faraday's law. This current gives information about the rate of the redox reaction and it can be visualized by means of a *voltammogram*, namely a plot showing current signal versus excitation potential. The total current includes faradaic currents for both sample and blank solution and the nonfaradaic charging background current. The rate of the reaction will be determined by the slowest step in the sequence, namely the most sluggish [20]. A reaction can be controlled by mass transport or electron transfer, depending on the type of compound measured and by experimental conditions [20]. Reactions are said to be nernstian or reversible when they are mass transport-limited, namely when they are only controlled by the rate at which the electroactive species reach the surface; they are called like this because they obey thermodynamic relationships [20].

In order for the interface to remain neutral and to compensate for the excess charge on the electrode, an *electrical double layer* (EDL) is formed. The EDL is discussed further in the appendix A.

1.2.2 Types of electrochemical sensors

Electrochemical sensors can be divided into various categories: amperometric, potentiometric, voltammetric and conductometric/impedimetric. **Potentiometric** sensors focus on the charge potential accumulated on the working electrode in comparison to the reference. In particular, the analytical information is obtained converting the recognition process into a potential signal logarithmically proportional to the concentration of the target analyte. This devices are characterized by low selectivities but they allow continuous, on-line and real-time monitoring; they are also portable and cheap devices [8, 19]. The **conductometric** configuration is instead used to measure the variation in the analyte conductivity owing to the number of charges generated in the electrolyte. These measurements are usually carried out by applying an AC potential. The conductivity is a linear function of ion concentration and it can therefore be used for sensor applications; these sensors are commonly used for pathogen detection [8, 19]. **Impendimetric** sensors are similar to conductometric ones, but instead of measuring the voltage, they measure the current due to an applied sinusoidal voltage. Impedance is computed as the ratio between voltage and current in the frequency domain [19]. In conclusion,

voltammetric sensors exploit voltammetry as an electroanalytical method, leading to a linear dependence of the current from the concentration of the electroactive species. The amperometric configuration is nowadays considered as a subset of voltammetry and it consists in the application of a constant potential between reference and working electrodes; the output current related to the redox reactions involving electroactive species is measured continuously. The current generated in the process is linearly related to the concentration of the target analyte. A drawback of this technique is the interference of the different electroactive compounds present within the sample [8, 19].

1.2.3 Voltammetric techniques

Going into the details of voltammetry, electrochemical reactions can be studied qualitatively by means of **cyclic voltammetry** (CV). It is a fundamental tool for the assessment of the electrocatalytic performance of electrodes and electron transfer and it usually involves a three-electrode system (reference, counter and working electrodes) [19, 12]. It consists in the linear scanning of the potential of a stationary working electrode in an unstirred solution by means of a triangular potential waveform, as shown in figure 1.5 (a). During this process, the resulting current is measured by means of a potentiostat: the final result is a plot current (y axis) versus potential (x axis) called *cyclic voltammogram* and shown in figure 1.5 (b). The positions, shapes and relative peak amplitude of the redox peaks in the cyclic voltammogram are determined by the electron transfer rate and chemical stability of the analyte. The oxidation of the NTs at the electrode surface generates an oxidation peak; its amplitude is higher for a higher concentration of analyte in the solution. The target analyte concentration can be directly estimated from the peak current [12, 19].

This method can provide information about the thermodynamics of the redox processes, but also on the kinetics of heterogeneous electron-transfer reactions and on coupled chemical reactions or adsorption processes. It is able to provide a rapid location of redox potentials of the electroactive species and to evaluate the effect of media in the redox process. Considering figure 1.5, it is possible to understand the procedure. At the beginning, only the oxidized form is present (O): the cycle starts from a potential where reduction does not occur and it is characterized by a negative potential sweep. This half-cycle is the one scanning the region in which the reduction process takes place. The cathodic current starts to increase as soon as the potential applied to the electrode reaches the characteristic E^0 for the process, until a peak is reached. The second half of the cycle will explore the oxidation process. The direction of the potential is reversed, allowing the R molecules generated in the previous half-cycle and accumulated near the surface to oxidize into O again: an anodic peak appears. The change in the concentration

gradient with time affects the current peaks, as they are due to the formation of the diffusion layer. As a consequence, the change in the surface concentration modifies the diffusion layer thickness, leading to a change in the current peaks. As the peak current increase, diffusion control is achieved [20]. Cyclic voltammetry can be exploited for quantitative applications as well, when the peak current is measured. In this case, a baseline has to be set in order to compute the peak current [20].

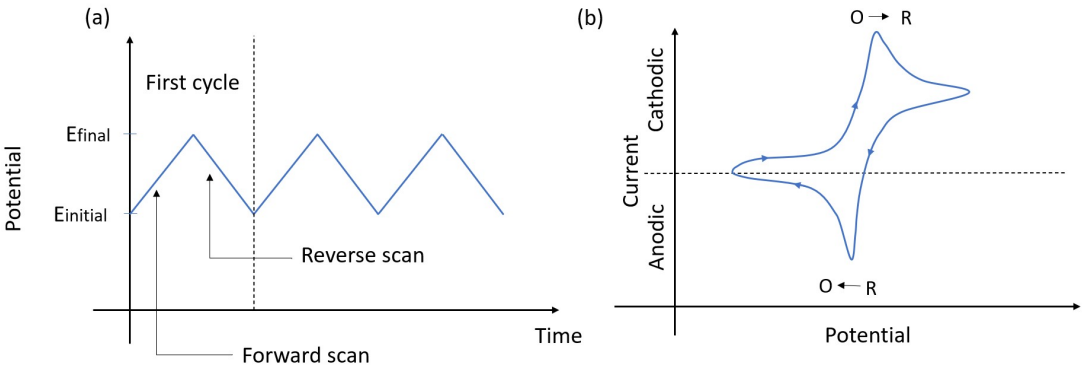

Figure 1.5: (a) excitation signal for CV (b) Cyclic voltammogram for reversible redox process

In order to lower the detection limits of voltammetric measurements, **pulse voltammetry** has been introduced. Such technique can reach $10^{-8}M$ concentrations by increasing the ratio between faradaic and nonfaradaic currents and it enables multi-analyte detection with a single probe [12, 20].

All the pulse voltammetry techniques are based on chronoamperometric experiments, namely sampled current potential steps. Each potential of the sweep is applied to the working electrode for a fixed amount of time: after the potential is stepped, the charging current exponentially reaches a negligible value, while the faradaic one decays more slowly. As a consequence, faradaic and charging currents can be effectively distinguished as long as the sampling is carried out long enough after the the pulse change. Different pulse voltammetry techniques are characterized by the same working principle, but they exploit different excitation waveforms and current sampling regimes [20].

Going into the details of **differential pulse voltammetry** (DPV), its working principle can be explained. This technique can be used for measuring trace levels of organic and inorganic species. Differently from CV, the charging current is negligible when DPV is used, leading to an improved accuracy in the measurement

[20]. The working principle of such method consists in applying fixed-magnitude pulses to the working electrode one at a time, superimposed on a linear potential ramp, as shown in figure 1.6. Current sampling is carried out twice, before pulse application (number 1 in figure 1.6) and at in late life of the pulse (number 2 in figure 1.6). After the sampling, the current recorded in 1 is subtracted from the one measured in 2: the current difference is plotted against the potential applied on the working electrode. The differential pulse voltammogram shows peaks in the current corresponding to each analyte: the height of each peak is directly proportional to the concentration of the corresponding analyte [20].

Different species can be identified by means of the peak potential (E_p):

$$E_p = E_{1/2} - \frac{\Delta E}{2} \tag{1.3}$$

Thanks to the peak-shaped response of differential pulse voltammetry, species with similar redox potential can be distinguished with a higher resolution. It is important to point out that pulse amplitude and potential scan rate selection requires a trade-off among sensitivity, resolution and speed [20].

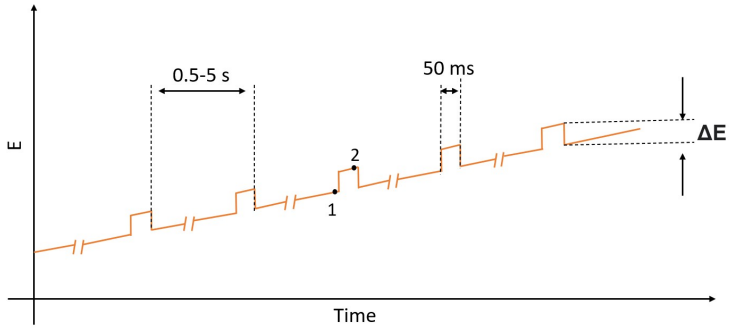

Figure 1.6: Excitation signal used in DPV

1.2.4 Electrochemical (bio)sensing

Electrochemical techniques can be exploited in biosensing in order to transduce the concentration of a biological analyte into an electrical signal. These sensors are relatively cheap and rapid, making them useful in many fields, including healthcare, environmental monitoring and biological analysis. For electrochemical sensing, the electrode will be considered to be the transducer and it can be easily miniaturized [19].

Focusing on the detection of NTs, one must note that electrode modification plays a key role in the enhancement of the sensor's performance. It can be carried out by means of biomolecules for target recognition (enzymes, antibodies or aptamers), or by other materials, such as MIPs or nanomaterials [6]. In addition, a signal transduction mechanism should be chosen in order to indicate the binding event under analysis [6]. As DA can be easily oxidized, electrochemical sensors are the best option for its detection [7]. Furthermore, DA is an electroactive molecule and, as a result, it does not require any enzyme to be detected [17].

Once again, it must been bore in mind that neurological biomarkers are characterized by extremely low levels in biological fluids. As a result, ultra sensitive detection methods are needed to detect them. The electrode surface is usually modified to improve selectivity, sensitivity and accuracy of (bio)sensors [3, 19].

Several biochemical species in the brain are characterized by similar oxidation-reduction potentials: biosensors easily face difficulties in the detection of NTs in the presence of interfering species. As a consequence, selectivity is a vital property in a sensor for NTs [12]. Such intereferents, ascorbic acid (AA) and uric acid (UA) in the case of DA, are often present at orders of magnitude higher concentrations with respect to the target NTs [21].

Another challenge of NT detection is their fast release and uptake (DA in particular) at the neuron terminals. It is therefore extremely important for the sensor to be characterized by a fast response [17].

Last, it is important for a NT sensor to be biocompatible and resistant to biofouling: the electrode material is therefore a key parameter in the development of sensing strategies for NTs. These properties are required for in vivo sensing and they allow the sensor to remain stable and reliable [17].

One of the most important characteristics of biosensors is miniaturization, as mentioned above. The miniaturization of electrodes to micrometric scale ensures the packing of many trasducers onto a small biochip device, leading to portable high-density arrays. Miniaturisation enables the *in vivo* real time monitoring of electroactive species, as it improves, among other things, the sensitivity of the sensor. Microelectrodes exhibit higher temporal resolution and current densities, lower ohmic drop and charging currents and high faradaic to capacitive current ratios. Their individual output is shadowed by the electrochemical noise and, for this reason, micro-electrode arrays (MEAs) have been developed; MEAs are able to improve the sensitivity and making detection limits lower compared to macro-electrodes. They are widely used for NTs detection *in vivo*, as they make the electrode-neuron communitation easier. The exploitation of new materials, such as carbon nanotubes, has brought about the most significant improve in the operation of microsensors; the research is going towards the fabriaction of lab-on-a-chip devices, making the sensing process much simpler, cheaper, but also disposable, scalable and easy to use [2, 19].

1.2.5 Sensor properties

Let us now consider some of the static properties of sensors: such properties characterize the sensor after the transient effects have been stabilized to their steady state values. Some of the following properties can be evaluated from the calibration curve, which represents the relationship between the measured variable (x) and the signal output generated by the sensor (y). This is useful to be able to calibrate the sensing system with respect to a known measurand, in order to ensure the correctness of the outputs [22].

- **Accuracy**
  The accuracy of a sensor represents how good is the obtained result with respect to the true value of the measurand. In order to obtain this evaluation, the result from the sensor should be compared either to a benchmark value or to the result from a more accurate instrument [22].

- **Repeatability**
  Repeatability represents the ability of the sensor to return the same response for successive measurements if the operating and environmental conditions are constant. It can be evaluated both long term and short term [22].

- **Minimum Detectable Signal (MDS)**
  It is the minimum signal increment that can be observed. If the increment is computed starting from zero, then the value can be also reffered to as limit of detection (LOD) [22].

- **Sensitivity**
  The sensivity of a sensor is the ratio of the incremental change in the output of the sensing system (Δy) to the incremental change of the measurand (Δx). It can be computed as the slope of the calibration curve for a given analyte. An ideal sensor would be characterized by a constant and large sensitivity in the operating range. The sensor will in turn reach a saturation state in which changes in the measured variable do not affect the output anymore. A sensor has got a good sensitivity when a small change in the analyte concentration leads to a large change in the response [22].

- **Linearity**
  Linearity evaluates how close the calibration curve is to a straight line [22].

- **Selectivity**
  Selectivity is the capacity of the sensor to measure a detection target when other species are present [22].

1.3 Conducting polymers

1.3.1 Introduction to conducting polymers

Polymers are generally considered to be insulators, although some of them are found to be conductive. Conducting polymers (CP) are a class of organic materials with unique electrical and optical properties, similar to the ones characterizing inorganic semiconductors. They can also be referred to as *conjugate polymers*, as they are characterized by conjugated carbon chains made of alternating single (σ) and double (π and σ) bonds. Figure 1.7 shows the structure of polyacetilene, which has been chosen for its easy structure and high conductivity. Both single and double bonds in the skeleton of the CP contain a localized σ bond, which provides a strong chemical bond; the π bond contained in the double bonds is instead weaker [23, 24].

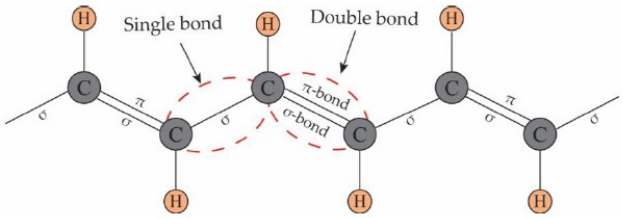

Figure 1.7: Structure of polyacetilene [23]

This structure allows charge carriers to be strongly delocalized in polarized π bonds. Delocalization is fundamental for the generation of nonlinear local excitations, including polarons, bipolarons and solitons, which are stricly related to the transition from the insulator to the metallic state. In conclusion, delocalization appears to be the reason why CPs possess such particular properties [23, 24].

Due to the alternating single and double bonds, CPs show a lower number of monomer units with respect to conventional polymers, which need thousands to millions of them [24]. Solubility and processability of CPs is mostly due to the presence of different side chains, while the attached dopant ions affect their mechanical, electrical and optical properties. Pure CPs behave in fact like insulators or semiconductors and their conductivity is increased thanks to the doping. Similarly, mechanical and optical properties of pure CP can be related to those of conventional semiconductors with anisotropic, quasi 1D electronic structure [24]. When the polymer undergoes doping or photoexcitation, in fact, the π bonds experience self-polarization, leading to the nonlinear excitation of polarons, solitons and so on; at this point, the polymer turns a nonlinear excitation state into a metallic one [24].

CPs are mostly crystalline, but also partially amorphous. They show both localized and delocalized states: the delocalization of the π bonds is mostly depending on the disorder [24].

In the following list the characteristics making CPs particularly interesting are summarized:

- Tunable electrical properties
- Outstanding optical and mechanical properties
- Easy synthesis and fabrication: shape and morphology are easy to control
- High environmental stability with respect to conventional inorganic materials and corrosion resistance
- Chemical diversity
- Low density
- Flexibility

At the same time, CPs are affected by a large amount of limitations, which can anyway be overcome by the hybridization of the material. A few of the backdowns characterizing conjugate polymers in their pure form are the low conductivity, poor optical properties, solubility and long-term stability. In order to solve such problems, CPs can be modified or hybridized. For example, doping with suitable materials can be employed, leading to excellent properties. Another interesting way of modifying CPs is the hybridization with carbon nano-species, as it will be investigated in section 1.5 [23, 24].

1.3.2 Applications in sensing technologies

An interesting electrochemical property of CPs is the reversible oxidation and reduction. Doping is a cause of geometrical changes in the structure of the CP, for example from benzoid to quinoid; the reduction of the polymer has the power to recover the structure of original undoped state. This doping/de-doping process is related to the charge/discharge mechanism undergone during a redox process [23].

CPs have also recently been employed in sensing technologies. This kind of sensors rely on the change of CPs capacity, optical properties or redox properties, for example; the sensitivity of the sensor will be given by the difference of the property before and after the exposure to the target molecule. The variation of the conductivity caused by the doping/de-doping process is often used for sensing purposes, as target molecules can change both the number and the mobility of charge carriers upon binding, leading to a change in conductivity [25]. CPs also

represent a turning point in electrochemical sensing, as they are characterized by fast response time, recovery time and low operational temperature: the latter advantage allows these sensors to be used at room temperature, providing them with a longer life. Conventional electrodes are usually made of metal oxides and inorganic materials, but they require higher operational temperatures [24].

CPs are often used to modify electrochemical sensors in order to improve their sensitivity, selectivity and reliability. They are often deposited on the electrode surface by means of electrodeposition, leading to an increase in the catalytic activity of the electrode. Unfortunately, CPs are characterized by low sensitivity and reliability, as the electron transfer between the target molecule and the current collector is quite poor. In order to solve this problem, carbon-based nanomaterials are widely employed in the fabrication of electrochemical transducers, as they ensure better electron transfer thanks to their good properties. Carbon nanomaterials are in fact characterized by high conductivities, inertness, wide voltage range and fast heterogeneous electron transfer [12, 23].

1.3.3 Examples of CPs and focus on PPy

Some of the most famous conducting polymers are listed below:

- Polyacetylene
- Polyaniline
- PPy
- Poly(p-phenylene)s
- Poly(p-phenylene vinylene)
- Polythiophenes

PPy, whose molecular structure is shown in figure 1.8, was first discovered to be a CP in 1968 and it is widely used in many different application, especially in sensing technologies [26].

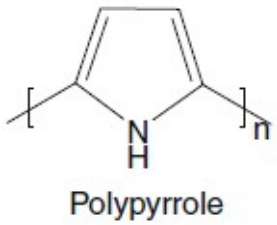

Figure 1.8: PPy molecule [25]

PPy has been widely studied among the other CPs, mainly because of the properties listed below:

- Superior electrochemical properties, as rapid electrochemical response [27]
- Good magnetic, optical and mechanical properties [26]
- Stabilized oxidized form [26]
- Easy and quick preparation [18]
- Partial cross-linking behaviour: there is no need for a cross-linking agent [18]
- Good behaviour in neutral pH [18]
- High electrical conductivity, environmental stability and biocompatibility [18]
- Low cost and commercial accesibility [27, 26]

PPy can be polymerized by means of electropolymerization on the surface of metallic electrodes [27].

Pristine PPy behaves as a semiconductor, with a band gap of 3.16 eV. When p-type doping is applied, the backbone undergoes oxidation and π electrons are lost: this induces a deformation in the polymer structure, which goes from benzoid to quinoid and generates a polaron. The polaron creates a localized electronic level in the band structure; further oxidation to bipolarons might occur when π electrons are removed. This new state is able to reduce the band gap from 3.16 eV to 1.4 eV, inducing the transformation from semiconductive polypyrrole to metallic PPy [24].

PPy is a very interesting CP for electrochemical sensing applications, as its electrochemical properties are extremely good. It indeed provides wide dynamic range and low detection limits and it can be exploited for the determination of both low and high molecular weight species [7, 27].

Furthermore, CPs could be exploited as MIP in electrochemical sensing technologies thanks to several advantages they present. First of all, they allow to carry out imprinting at room temperature preventing therefore denaturation and conformational change. In addition, the template removal and the rebinding of the target molecule can be proved to be easy by electrochemical means. In conclusion, thanks to the formation of carbonyl and carboxylic groups into the PPy backbone, over-oxidation of PPy confers a perm-selectivity behaviour for electropositive groups of DA against anionic interfering species (like AA). As a result, polymeric coatings on electrodes allow an increase in selectivity, especially for DA over AA [7, 27, 28].

1.4 Molecular imprinting technology

1.4.1 Working principle of molecular imprinting

Molecular imprinting is a technique leading to the formation of synthetic polymers with selective sites to a particular analyte. Such sites are made by means of polymerisation of functional monomers in the presence of the analyte molecule: this is namely a template-directed polymerization method. Molecular imprinting is also a biomimetic strategy, as it confers the ability of living organism to synthetic polymers. This ensure high affinity and selectivity for the analyte molecule and high resistance to environental factors (temperature, extreme pH); MIPs can also easily regenerate themselves [14, 18].

Bio-materials can be incorporated into electrochemical sensors in order to improve their selectivity. Molecularly imprinted polymers attempt to mimic the selectivity of nature and, as a matter of fact, it is able to reach them. Other methods to increase the selectivity is the use of biomolecules, such as antibodies, nucleic acids and aptamers [19].

MIPs are used for selective binding and they are achieved by means of a cocktail solution containing the following elements:

- **Template molecule (target)**
  It is the molecule of interest and cavities complementary to its shape and functional group will result from the imprinting process. It is required to have good chemical and physical interaction with the functional monomer. Not every molecule can be used as template for molecular imprinting due to stability at high temperatures, presence of polymerizable groups or presence of groups inhibiting the polymerization [15].

- **Functional monomers**
  The functional monomer forms the the backbone of the structure emerging after polymerization. It is important for the functional monomer to possess a functionality that increases the chances of interaction with the template molecule: this provides active memory sites on the MIP. Some functional monomers, such a pyrrole, are also called "crosslinking monomers", as they are able to cross-link thanks to their large number of functionalities; this reduces the cost of molecular imprinting and improves the rebinding process [15].

- **Crosslinker agent**
  Crosslinking in the polymers is a vital parameter for the mechanical stability of the resulting MIP, as well as its morphology and the stability of the binding sites. Therefore, the cross-linking agent is much more abundant then the functional monomer in the initial mixture, leading also to a macroporous morphology. Furthermore, functional monomer and crosslinker need to be

characterized by a good chemical interaction: this ensures a stable network after polymerization [15].

- **Porogenic solvent**
  Such solvents are used for bringing all the components to into a single phase and they allow the formation of pores in macroporous polymers, controlling the morphology of MIPs. Good porogenic solvents are able to provide the MIP with favourable surface area, pore structure and size. In addition, the solvent should support the pre-polymerization complex formation in the MIP sinthesys [15].

- **Initiator**
  They can be triggered thermally or photochemically in order to obtain free radicals. This works for example when low temperatures are required: in this case, a photochemically triggered initiator can be exploited for the process [15].

The target molecule, the monomers and the cross-linker are dissolved into a solvent, together with the other elements. A highly cross-linked polymer is formed thanks to the new bonds between template and cross-linked polymer during curing process. After the polymerization, the template molecules need to be removed and, by doing so, nano-sized cavities complementary to DA are left behind. Their size, shape, orientation and chemical interactions are the same corresponding the template itself [7, 18].

The process described above has been shown in figure 1.9.

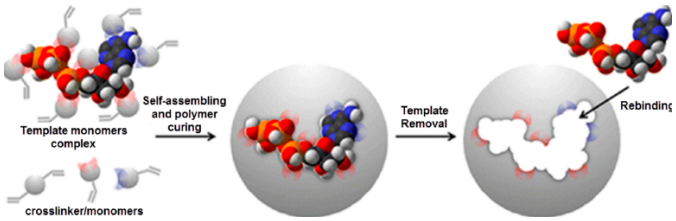

Figure 1.9: Graphical representation of the molecular imprinting process of a polymer [29]

The template is the critical molecule in the process, while the other elements are chosen depending on the chemical and physical properties of the target itself. It is also important to point out that the strength of the imprinting is optimized varying the monomer and cross-linker ratio in the initial cocktail solution [29].

1.4.2 Resistance in molecular imprinting

MIPs are denoted by an insulating behaviour: after the template has been removed, the resistance undergoes a drop due to the discharge of the template molecules. This is a useful way to determine wether the "washing" of the polymeric film has been carried out correctly [14].

Figure 1.10 shows the evolution of impedance in the imprinting process. Looking at the figure, an impedance change is recorded when the MIP has been deposited on the surface of the electrode (curves **a** and **b**); in particular, the resistance tends to increase as the polymeric film acts as an insulating layer. This layer blocks the electron transfer between the electrode and the electrolyte during the study. The resistance decreases again when the template is removed from the cavities (curve **c**): electrons are once again able to conduct. Resistance increases again once the MIP has interacted with the target: the cavities are filled again and the electron transfer is reduced once more (curve **d**) [27].

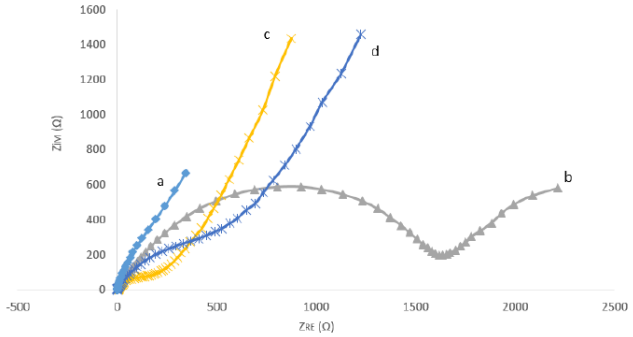

Figure 1.10: Impedance change during the imprinting process, (a) bare electrode, (b) MIP modified electrode before template removal, (c) MIP electrode after template removal, (d) MIP electrode after interaction with target [27]

1.4.3 Parameters to optimize

Several parameters are to take into account when carrying out molecular imprinting; they are introduced in the following section and they will be treated in chapter 2 from the practical point of view.

An interesting parameter in the molecular imprinting process is the **template concentration**. It has been found that the template concentration is directly proportional to the number of recognition sites in the MIP and therefore, as the concentration increases, the peak current increases as well [27].

Another parameter to take into account is the **number of cycles** set for the electropolymerization process, which can be for example carried out by CV. This

is stictly connected to the thickness of the polymeric layer deposited onto the electrode, which can affect the response of the MIP sensor. As the thickness of the polymeric layer increases, it can become difficult to reach the imprinted sites due to mass transfer resistance. Once more, this step has been optimized and described in the results section [27].

In addition, it is important to consider also the **pH of the imprinting solution** as a parameter to optimize. The pH has a strong effect on the target oxidation on the surface of the modified electrode, leading to a change in the electrode performance. This parameter as well has been optimized and analysed in the following sections [27].

At last, another important parameter is the **incubation time**. After template removal, the MIP electrode can be used to detect the target: if the electrode is left in the solution containing the target for some time, the performance might increase. A maximum incubation time can be found and used in order to optimize the performance of the electrode [27].

1.4.4 Why molecular imprinting?

The performance of the detection methods for neurotransmitters are generally affected by some interfering molecules. In catecholamine detection, the most important interfering species are considered to be AA and UA, which coexist with DA in biological fluids: their oxidation peaks overlap with the one for DA, which would be shaded, leading to a lack of selectivity. Molecular imprinting technology is an interesting solution for this problem, greatly improving the selectivity of the sensor. The cavities are able to provide memory binding sites for the target molecule, providing a natural way to cancel or strongly reduce the competition with the interferents [15, 18]. Focusing on carbon-based electrodes, it has been proved that many of them are able to reach extremely good sensitivities even though selectivity is still a challenge [21]. Molecular imprinting is helpful in the enhancement of the selectivity of the electrodes, improving their performance [15, 18].

Molecular imprinting is also able to counter the passivation of the surface of the bear electrode due to the formation of an unwanted polymeric film on it; this problem is a consequence of the further reactions of catecholamines in the solution [15, 18].

It can be proved that MIPs are better than their non-imprinted counterparts, as they allow a larger current. This is a way to estimate the improved selectivity of MIPs based electrodes, and it will be discussed later on [15]. This discussion holds particularly well for the detection of catecholamines: thanks to the molecular imprinting, superior selectivity can be achieved. It is therefore important to point out that the traditional oxidation of catecholamines is still taking place on the

surface of the MIPs based electrodes. The difference between unmodified electrodes and MIPs electrodes lies in the fact that, in the second case, analyte molecules are encouraged to migrate in a discriminatory way, owing to the presence of the cavities [15].

1.4.5 Advantages and disadvantages

Table 1.3 provides a schematic description of the advantages and disadvantages of MIP-based sensors.

Advantages	**Disadvantages**
Great selectivity	Low sensitivity
Low cost	Difficulties with macromolecules imprinting
Robustness	Lower affinity and specificity than biomolecules
High recognition ability	
Long term durability	
Increased chemical and mechanical stability	
Lower cost and higher stability than biomolecules	

Table 1.3: Advantages and disadvantages of MIP-based sensors

The advantages of MIP-based electrodes allow them to be exploited in many different biotechnological application fields [29]. The great selectivity of MIPs, for example, paves the way to applications in clinical analysis, medical diagnostics, environmental monitoring and drug delivery [18]. Furthermore, thanks to their chemical stability, MIPs are resistant to organic solvents, extreme pH and autoclave treatments, which further increase the possible application fields [29].

Comparing MIPs with biological receptors, their low cost and stability make them better as sensor materials. In fact, enzyme-based sensors for DA, for example, are characterized by good specificity, but they are also difficult to purify, less stable and they need complex immobilisation process. Considering instead antibody-based sensors, they are usually slow and not very sensitive to DA and therefore they are not considered to be competitive. MIPs show instead good specificity, low cost and high stability; they can also be combined with nanomaterials to improve sensitivity and specificity even more [7].

1.5 Surface modification: carbon nanomaterials for electrochemical sensing electrodes

Carbon is a very flexible material, as its unique properties could be easily tailored for a specific purpose. Carbon exists in fact in several different allotropes, from one dimensional to three dimensional structures [5].

By definition, a nanomaterial is characterized by at least one dimension smaller than $100\,nm$; their application to electrochemical sensing has its roots in the 1990's [30]. Nanomaterials are characterized by unique properties compared to their bulk forms, thanks to the reduced dimensionality [5]. Carbon-based nanomaterials have collected great interest from the scientific comunity for applications in biomedicine also thanks to their unique chemical and physical properties. The existence of a large number of allotropes contributed to their popularity, as each of them exhibits unique properties applicable in many different fields, such as biosening, drug delivery and tissue engineering [31].

Hybrid carbon nanomaterials are instead considered to be integrated structures where different carbon allotropes are combined together: the production step allows the strong bonding between the materials or generates a new material [30]. Carbon hybrid nanomaterials have been defined by Laurila et al. as a material integrating two or more carbon allotropes, which properties are significantly better than those of its components. Furthemore, its fabrication method should be controllable and repeatable in order to allow miniaturization [5].

Carbon nanomaterials have been a very popular research topic over the past years, leading to an improvement in the fabrication techniques regarding them: nowadays they can be made by nanolithography and 3D printing [28].

In addition, nanometerials are generally characterized by excellent conductivity, sensitivity to ligand binding and biocompatibility [7].

One of the way to classify carbon nanomaterials can be according to their dimensions [32]:

- 0D: spheres and clusters
- 1D: nanofibres, nanowires and nanorods
- 2D: films, plates and networks
- 3D: nanoparticles

Another classification criteria might be depending on their chemical structure and, in particular, through the carbon allotropies [28]. The most investigated carbon nanomaterials for electrochemistry are the sp^2 hybridized ones. This family of materials is characterized by extended conjugation, electron delocalization and high electronic conductivity. Among the most popular sp^2 hybridized carbon

nanomaterials there are carbon nanotubes (CNTs), especially for microelectrode fabrication [28]. An example of an sp^2 material is graphene, which is a sheet of sp^2 hybridized carbon atoms and is characterized by high conductivity due to its extended conjugated system. A perfect sheet is mostly made of the basal plane, which does not provide great adsorption; for this reason, graphene oxide is often exploited. However, it is complicated to use one single graphene sheet and, as a consequence, its 3D forms are often preferred [28]. The other family of carbon allotropes can be considered to be sp^3 hybridized materials. Although the sp^3 hybridized form of carbon, namely diamond, is an insulator, conductivity and electrochemical activity can be achieved upon nanostructure fabrication and doping [28]. Ta-C, which will be further described below, is an sp^3 hybridized amorphous carbon structure. Its synthesis is compatible with nanofabrication and it can be easily fabricated as a thin film on a silicon substrate. This material has been widely used for DA detection, as it was found to be highly responsive to it [28].

1.5.1 Amorphous carbon

Amorphous diamond-like carbon (DLC) is a non-cystalline material characterized by a high fraction of diamond-like sp^3 bonds [1]. Amorphous carbon (a-C) is a disordered material usually generated as thin film; it is advantageous with respect to its crystalline form due to the possibility to deposit it at room temperature, among all. Different properties and different degrees of disorder can be obtained with different deposition parameters and techniques. Its easy processability and compatibility with current complementary metal-oxide semiconductor (CMOS) processes make a-C a desirable material [33].

DLC properties are strongly dependent on the ratio of sp^2 and sp^3 bonds, the amount of hydrogen, and the deposition method [34]. In general, DLC coatings are characterized by outstanding physical properties, such as hardness, high elastic modulus and mechanical robustness. They are also chemically inert to acids, alkaline solutions and organic solvents. Some other properties of a-C can be considered to be corrosion and wear resistance, low friction coefficient, low roughness and surface energy [1, 33]. Furthermore, a-C is also characterized by a wide potential window and by a low background current [21].

The reduced dimensionality of a-C surfaces brings about a change in their structural properties with respect to its bulk form. First of all, the fraction of surface sp^2 carbon atoms is much higher in 2D materials with respect to 3D ones. As a consequence, surface-localized electronic states with a π character are introduced and the DOS in the pseudogap is increased [5]. Furthermore, the aromatic character of sp^2 bondings on the surface is much more common than in the bulk material [5]. The unique properties of ta-C clearly originate from the features of the material's thin film form, as the fraction of sp^2 to sp^3 bonds [21].

Ta-C is a disordered carbon material characterized by a high fraction of sp^3 bonding, in particular between 60% and 85% [33]. The toxicity of a-C has been studied and it has been found that cells grown on different types of a-C, included ta-C, proliferate without any problems. In particular, a-C is able to favour the adhesion of cells with respect to a control sample. This implies a good biocompatibility of a-C, leading to interesting applications for *in vivo* measurements as well [33]. The interest on ta-C for *in vivo* applications is also due to its good mechanical properties and its resistivity to bacterial adhesion and fouling [21].

As mentioned, ta-C is extremely attractive as an electrode material, thanks to its antifouling properties [1, 21]. Biofouling is the main reason for sensor failing *in vivo*, as it reduces analyte diffusion and perfusion in implanted sensors. It consists in the passive adsorption of proteins and lipids from the medium, leading to the worsening of the analytical characteristics of the sensor and its very reliability [35]. In order to prevent biofouling, protein adsorption should be reduced or prevented. Strategies aiming to this include the involvement of protective layers on the electrode substrate, which should prevent the fouling agent to reach the electrode surface. Unfortunately, these barriers increase the background current and act as diffusion barrier, compromising the reaction kinetics of the electrode and, in turn, sensitivity and temporal resolution [35]. DLC electrodes have been found to be resisting much better to biofouling than other carbon materials, such as glassy carbon (GC), when soaked in bovine serum albumine (BSA) [36]. Thanks to the properties mentioned above, a-C is of great interest for biocompatible electrochemical sensors for *in vivo* analysis [5].

It has been found that the thickness and the roughness of the ta-C film deposited on the sensor surface are fundamental to enhance the performance of the sensing electrode. Rougher and thinner films ensure a better performance in DA sensing, as they show a higher conductivity. This films show a broadened water window, as well as fast electron transfer at the electrode/solution interface [1].

Unfortunately, the sensitivity of ta-C towards DA, for example, is not very high; for this reason, it is important to improve the performance of these electrodes by means of molecular imprinting, for example, as discussed in section 1.4 [1].

DLC electrodes are extremely stable in phosphate buffer saline (PBS) solution and they can be used for the detection of biomolecules inducing electrochemically active spots locally, as they are reported to be inert otherwise [1].

1.5.2 Carbon hybrid nanomaterials

Based on their definition, carbon hybrid nanomaterials can be considered to be even more versatile: the combination of different allotropic forms at nanoscale allows the fabrication of tailor made surfaces with tunable properties [5]. In particular, the combination of two or more carbon allotropes might lead to the creation of

hybrids with unforseen properties. The advantages of combining different carbon allotropes can be summarized in the following [5]:

- Nanocarbon materials can form a feasible interface with biological elements, being especially helpful in biomedical engineering;
- Carbon will most unlikely become a critical material, as it is extremely abundant in nature;
- Carbon nanomaterials possess excellent physical and chemical properties and they could be engineered to obtain the perfect combination of properties for the application under study.

Focusing on ta-C, it has been shown that it can host hybrid carbon structures, leading to extremely high selectivity and sensitivity values towards DA [17].

1.5.3 Electrochemical detection of neurotransmitters

The application this discussion focuses on is the electrochemical detection of NTs and DA in particular. NTs are difficult to detect both due to their low physiological concentrations and co-presence with several interfents: sensitivity and selectivity are therefore a challenge [5].

Due to the above-mentioned reasons, electrode modification is key to the achievement of high performance voltammetric sensors for the determination of NT, and DA in particular. From a general stand point, modification is aimed at the improvement of the electron transfer rate, undesired reaction prevention and sensitivity and selectivity enhancement. Nanomaterials, thanks to their high surface-to-volume ratio, provide the modified electrode with high electron transfer rate and improved selectivity and sensitivity [32].

Carbon nanomaterials have been extensively used for the modification of electrodes for neurotransmitters detection, thanks to their important properties. First of all, they provide surface roughness and improve the absorption of DA, among all [28]. In addition, the large active surface area and good electrocatalytic activity they provide is able to improve the performance of electrochemical transducers [12]. Thanks to their properties, carbon-based nanomaterials are usually characterized by excellent conductivity, sensitivity and biocompatibility, which make them great candidates for electrode modification in DA detection [7, 19]. In addition, incorporation of nanostructures into the sensors allows the improvement of signal-to-noise ratio (SNR) for a given analyte thanks to the increased electrode reactive surface area and less materials needed for the electrode [19].

Some basic electrochemical properties are strongly affecting the performance of sensors when carbon allotropes are considered. The width of the potential window, dependent on the material, affects the range of analytes that can be detected: a

wide potential window allows the measurement of a larger number of species. The double layer capacitance acts on the performance of the sensor as well: when it is small, the background current is reported to be low as well, enabling the detection of smaller current peaks and lower analyte concentrations [5].

Another parameter affecting the performance of the electrode is the structure of its surface. If a 3D structure is chosen, it could increase the surface area and enhance the detected current; sensitivity is improved as a consequence. Furthermore, the roughness of the surface (or pores, for example) induces the temporary trapping of target molecules for the redox processes, helping the NT detection [28].

It has been found that selectivity can be improved when nanomaterials are combined with polymeric coatings [28]. The two main polymer categories used with this purpose are charged polymers and CPs [28], which have been exploited in the present study. Conducting polymers, which have been described in section 1.3, are characterized by advantageous properties, which make them easy to fabricate as electrode materials themselves or be deposited on electrodes to enhance sensitivity [28]. Carbon nano-species are in fact used for the hybridization of CPs, as they are able to enhance the structural order of the polymeric chains: this leads to an improved carrier delocalization and, in turn, to an increased conductivity [23]. Molecularly imprinted CPs, described in section 1.4, lack of conductivity, which brings about poor sensitivity and LOD. Nanomaterials have therefore been introduced into the fabrication of MIP-based NT sensors in order to improve the sensitivity, LOD values and linear concentration ranges [18].

1.6 State of the art: electrochemical MIP sensors for dopamine detection

In the following pages, the most recent MIP-based electrochemical sensors for the detection of DA were analysed.

Figure 1.11 shows the building blocks a NTs sensor. In the present case, the building blocks chosen were the following:

- Type of nanomaterial: ta-C
- Type of (bio)sensor: electrochemical
- Type of (bio)sensor modification: MIP imprinted PPy

Nanomaterials were often used for electrode modification for direct DA detection, thanks to their great conductivity, sensitivity, biocompatibility and the other properties mentioned in section 1.5. Electrochemical sensors have been proved to show enhanced performance when nanomaterials and MIP are coupled [7]. Many recent MIP-based sensors for catechol and catecholamines detection exploited electrochemical techniques, due to the excellent advantages discussed in section 1.2 [15].

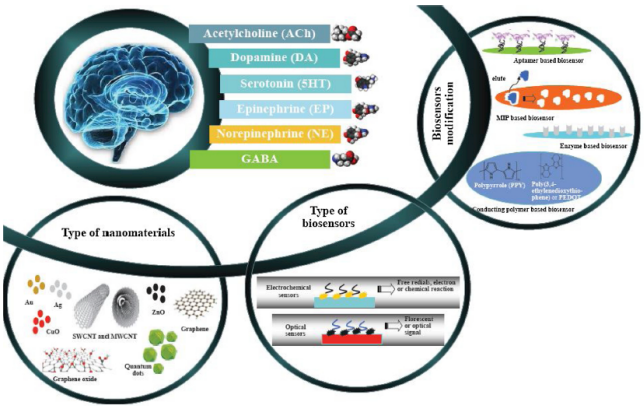

Figure 1.11: Building blocks of a sensor for NTs detection [6]

Among the MIP-based electrochemical sensors developed in the recent years, Lu et al. considered an electrochemical sensor intended for the detection of both DA and chlorpromazine. The sensor was analysed by DPV and a LOD of $2.8\,nM$ was found for DA. Furthermore, reproducibility and selectivity were found to be high for DA. The sensor was tested for the analysis of human serum, urine and pharmaceutical samples [37].

Mohanan et Al. have developed a MIP-based sensing system for DA showing excellent affinity for the target analyte. The functional monomer used was 5-amino 8-hydroxy quinoline (AHQ), which was electrodeposited on a reduced graphene oxide (rGO)-modified glassy carbon (GC) electrode and it was imprinted with DA. The affinity between between DA and the poly(AHQ) film enabled a high-performance detection of DA by means of CV and DPV techniques. The limit of detection and sensitivity of the GC/rGO/MIP electrodes were computed and found to be respectively $32.7\,nM$ and $13.3\,AM^{-1}cm^2$ [38].

Ermiş and Tinkiliç developed a sensor for the sensitive and selective determination of DA based on molecularly imprinted poly(p-aminothiophenol). The functional monomer was electropolymerized on a gold electrode in the presence of DA in order to build up the imprinted polymeric film. The performance of the electrode was studied through CV and electrochemical impedance spectroscopy (EIS), which showed an excellent behaviour compared to its non-imprinted counterpart. The LOD of the sensor was found to be $18\,nM$ and it was successfully employed in pharmaceutical samples [14].

The research from Song et Al. was based on a DA-imprinted chitosan (CS) film/ZnO nanoparticles (NPs)@carbon (C)/three-dimensional kenaf stem-derived macroporous carbon (3D-KSC) for the fast, efficient and sensitive determination of DA. The molecular imprinting was carried out by means of electropolymerization. The electrodes under analysis were studied by means of CV and DPV techniques and they were indicated to show a LOD of $0.039\,nM$[39].

Si and Song discussed the use of MIP-based electrochemical sensors for the selective detection of multianalyte NTs. The functional monomers taken into account in this study were pyrrole and o-phenylenediamine (o-PD) and they were electropolymerized on the electrode's surface. The electrodes were studied by means of DPV and they showed selective detection of DA and other NTs. The selectivity of MIP-based sensors was found to be higher than the one for non-imprinted polymer (NIP) sensors thanks to their gained recognition sites. The current electrodes were also found to be suitable for multi-analyte detection. The o-PD was electropolymerized on the electrode's surface and the sensitivity of the electrodes was found to be $0.59\,\mu A/mM \cdot cm^2$ and the LOD was proved to be $3.97\,\mu M$. The same authors developed DA-imprinted carbon nanotubes (CNTs) modified PPy sensors for the detection of DA and other NTs. The polymer was deposited by oxidative chemical polymerization method and studied by CV. The LOD was found to be $7.972\,\mu M$ [40].

Kajisa et Al. worked on a DA-imprinted polymeric interface for DA detection by means of a potentiometric biosensor. The sensor designed was a field-effect transistor (FET) biosensor, which gold gate was modified with a DA-imprinted vinyl-PBA layer. The linear range was found to be between $40\,nM$ and $20\,\mu M$ [41].

Ma et Al. developed a novel electrochemical sensing platform for the detection

of DA based on molecularly MIP-decorated 3D-multi-walled carbon nanotube (MWCNT) intercalated graphene aerogel. The functional monomer utilized was PPy and it was deposited on the electrode's surface my electropolymerization in the presence of DA. The MWCNTs highly improved the electrical conductivity and electrochemical performance of the electrodes. In conclusion, the sensing platform as found to be both sensitive and selective to DA. The sensor was studied by means of CV and DPV and the LOD was found to be $1.67\,nM$ [42].

Yang and co-workers developed a MIP-based sensor coupled with nanoporous gold (NP4G) as a nanomaterial, which was electrodeposited on a bare gold electrode. The work describes a nivel on-off ratiometric electrochemica sensor for selective and sensitive determination of DA. The NPG provided signal amplification and high surface area for polythionine (pThi) and MIPs immobilization. The functional monomer used for molecular imprinting was pyrrole, which was deposited on the MIPs/pThi/NPG electrode by electropolymerization. The studies were carried out by CV and the electrodes were found to show outstanding selectivity and excellent reproducibility. The LOD was reported to be $0.1\,\mu M$ and the sensor was proved successuful in artificial cerebrospinal fluid [43].

In order to carry out clinical studies, *in vitro* analysis is suitable; *in vivo* is instead employed in the continuous monitoring for the assessment of the state of the disease in time. Unfortunately, *in vivo* monitoring requires more complex electrodes characterized by lower sensitivity and higher cost. For this analysis, electrodes are implanted or semi-implanted into the brain. Microelectrode probes are however characterized by several challenges, such as the improvement of their longevity, durability and damage prevention during implantation [12].

The previous results are summarized in tables 1.4 and 1.5.

Authors	Polymer	Working electrode	Deposition method
Lu et Al. (2020) [37]	Nicotinamide	Au/N-GOQDs/NiS2/BC/MIP/GCE	Electropolymerization
Mohanan et Al. (2018) [38]	AHQ	GC/rGO-MIP	Electropolymerization
Ermiş and Tinkiliç (2021) [14]	p-aminothiophenol	poly(p-ATP) modified Au electrode	Eelctropolymerization
Song et Al. (2019) [39]	Chitosan	ZnO NPs@C/3D-KSC integrated electrode	Electropolymerization
Si and Song (2018) [40]	PPy-CNT	o-PD-DA-MIP	Oxidative chemical polymerization method
Kajisa et Al. (2018) [41]	vinyl-PBA	FET Au gate electrode	Atom transfer radical polymerization
Ma et Al. (2020) [42]	PPy	MWCNT/GAs	Electropolymerization
Yang et Al. (2019) [43]	PPy	MIP/pThi/NPG	Electropolymerization

Table 1.4: Summary of the most recent MIP-based sensors modified by carbon nanomaterials for the detection of DA (1)

Authors	Electrolyte	Washing parameters	Performance
Lu et Al. (202) [37]	0.1 M PBS pH 6.8	DA was eluted by immersing the the electrode in a methanol-acetic acid solution and stirring for 12 min	LOD: 2.8 nM
Mohanan et Al. (2018) [38]	0.1 MPBS pH 7.4	Washing in 0.5 M H_2SO_4 for 2 hours	LOD: 32 nM Sensitivity: $13.3A/M \cdot cm$
Ermiş and Tinkiliç (2021) [14]	PBS pH 7.4	DA/MIP sensor was immersed in 1 M HCl and the removal was checked by CV	LOD: 18 nM
Song et Al. (2019) [39]	0.2 M PBS pH 7	DA was eluted immersing the film into an ethanol solution of 0.010 M KCl under continuous stirring	LOD: 0.039 nM
Si and Song (2018) [40]	PBS buffer pH 6	CV	LOD: 7.972 μM
Kajisa et Al. (2018) [41]	PBS pH 7.4	1. washing in methanol and water to remove the unreacted monomers and DA 2. Immersed in 0.1 M HCl and 50% methanol for 3 days	DLR: 40 nM to 20 μM
Ma et Al. (2020) [42]	0.1 M PBS pH 6	CV in PBS pH 6 until no significant redox peaks are observed	LOD: 1.67 nM DLR: 5 nM to 20 μM
Yang et Al. (2019) [43]	PBS pH 7	CV until the peak of DA had vanished	DLR: $0.3 - 100$ μM LOD: 0.1 μM

Table 1.5: Summary of the most recent MIP-based sensors modified by carbon nanomaterials for the detection of DA (2)

Chapter 2

Objective

The goal of this study was the electrochemical fabrication of novel, non-toxic, low-cost and high-performance DA imprinted PPy coated ta-C electrodes. A schematic of the electrodes created in shown in figure 2.1.

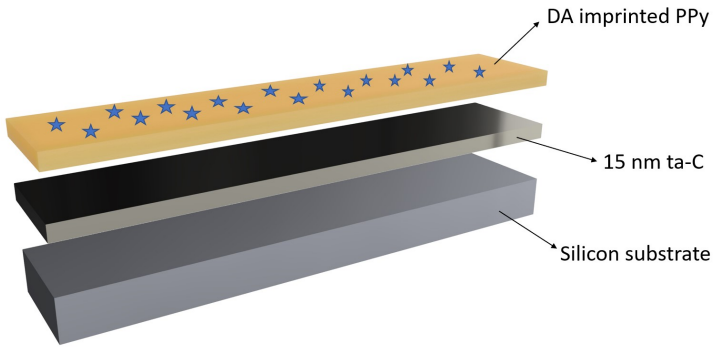

Figure 2.1: Schematic layer structure of the electrodes under study

The focus of the study has been to use molecular imprinting methods for the design of a sensitive and selective carbon-based electrochemical sensing platform for NTs detection and DA in particular. The performance of the electrodes has been investigated for DA in presence of other coexistent active molecules, such as AA, which are characterized by oxidation potentials very close to that of DA.

Based on the above-mentioned targets, ta-C has been studied both in its pristine form and modified for the detection of DA. The modifications taken into account are MIP and NIP on ta-C.

The performance of MIP/ta-C the new silicon-based sensors has been checked considering trace amounts of DA in physiological pH (around 7.4 in living cells).

The new electrochemical electrodes were fabricated and modified by means of MIPs, which provided an artificial recognition site for DA. The behaviour of the electrodes was evaluated electrochemically with CV and DPV, but also by means of other characterization techniques such as scanning electron microscopy (SEM), Raman spectroscopy and atomic force microscopy (AFM). The efficiency of the electrodes was tested for DA sensing in phosphate buffer saline (PBS) solution with physiological pH.

The main aims of the work are given in the following:

- Electrochemical synthesis of DA imprinted PPy on ta-C as a carbon based substrate
- Optimization of the molecular imprinting process, considering the following parameters
  - pH of the imprinting solution
  - Concentration of DA and pyrrole ratio in the imprinting solution
  - Number of cycle of the CV study
  - Scan rate of the CV study
- Characterization of the MIP/ta-C electrodes by using SEM, Raman spectroscopy and AFM
- Investigation of voltammetric behaviour of MIP, NIP and ta-C and comparison of their electrochemical bahaviour with CV
- Study of the performance of MIP, NIP, ta-C in presence of the target analyte (DA) and in plain PBS
- Study of the performance of the electrodes in the presence of an outer redox probe ($Ru(NH_3)_6^{2+/3+}$ in 1M KCl) by CV and comparison of MIP, NIP, ta-C
- Effect of incubation time on the sensitivity
- Effect of the potential scan rate (ν) on the response signal
- Performance of the electrodes in different analyte concentrations
- Performance of the MIP/ta-C modified electrode toward DA in presence of coexistent biomolecules such as AA, which has oxidation potentials very close to the one for DA
- Determination of LOD and dynamic range of DA concentration by using DPV

Chapter 3

Experimental

3.1 Materials and chemicals

- Copper
- Teflon
- Sodium chloride was purchased from Emsure ®
- Potassium chloride was purhased from Emsure ®
- Di-sodium hydrogen phosphate was purchased from Emsure ®
- Potassium hydrogen phospate was purchased from Emsure ®
- Dopamine hydrochloride was purchased from Sigma-Aldrich
- Pyrrole (98+%) was purchased by Alfa Aesar
- Hexaammineruthenium(III) was purchased from Sigma-Aldrich
- L(+)-Ascorbic acid was purchased from Emsure ®

3.2 Instruments

- Gamry Instruments Reference 600+ Potentiostat/Galvanostat/ZRA
- Gamry Instruments Reference 600 Potentiostat/Galvanostat/ZRA
- pH/mV/°C meter, bench, pHenomenal® pH 1100 L
- Zeiss Sigma VP (Entry-level SEM) - NMC
- Bruker Dimension Icon AFM
- WITec WITec alpha300 RA+ Raman Spectroscope

3.3 Solutions

All solutions were prepared with de-ionized water (DIW). The PBS solution was prepared mixing the following ingredients:

- 80 g Sodium chloride (NaCl)
- 2.0 g Potassium chloride (KCl)
- 14.4 g Di-sodium hydrogen phosphate (Na_2HPO_4)
- 2.4 g Potassium hydrogen phospate (KH_2PO_4)

The ingredients are diluted into 1 litre of DIW. The solution is now 1 litre of 10X PBS. When it is diluted with 9 litres of DIW the final pH should be 7.4, namely the physiological one. The pH can then be adjusted to the desired one by adding HCl or NaOH.

3.4 Methods

In order to characterize the electrodes, voltammetric studies were carried out with CV, DPV and EIS. They were performed with a conventional three-electrode system using both Gamry Instruments Reference 600+ Potentiostat/Galvanostat/ZRA and Gamry Instruments Reference 600 Potentiostat/Galvanostat/ZRA. The reference electrode used for most studies was a KCl-saturated Ag/AgCl electrode. A silver wire was instead employed as a reference electrode for imprinting and EIS studies. The counter electrode used was a platinum wire.

The samples were characterized by SEM, Raman spectroscopy and AFM. Instrumentation models are described in section 3.2.

3.5 Material fabrication

The material chosen for the electrode was silicon coated with ta-C as a carbon nanomaterial. The silicon used was a (100) highly conductive p++ doped silicon wafer. The ta-C was sputtered on the silicon wafer by physical vapour deposition (PVD). Two different samples were investigated: one without adhesion layer and another one with a titanium adhesion layer. The wafers were all cleaved by hand with the help of tweezers and a diamond pen.

In order to fabricate the electrodes, the materials required are listed in the following:

- Copper sheet
- Teflon tape
- Silicon wafer coated with ta-C
- Copper tool
- Diamond pen
- Piercer

A schematic of the resulting MIP/ta-C electrode is shown in figure 3.1.

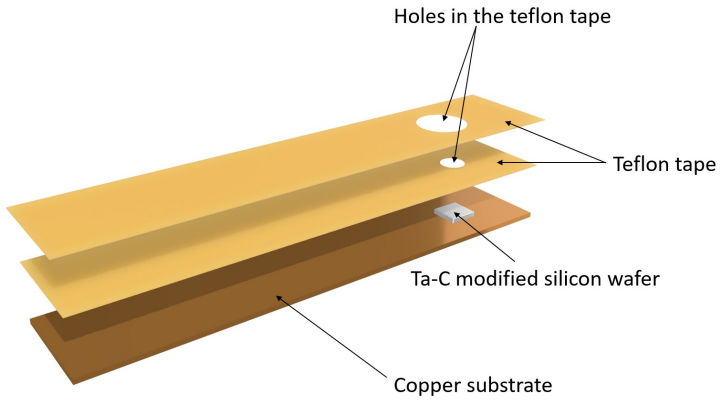

Figure 3.1: Schematic of the MIP/ta-C electrode

The process for the electrode preparation is described below schematically:

1. A short piece of teflon tape is first attached to a substrate (paper, for example) in order to be able to pierce it;
2. A piercer is used to cut a hole into the teflon tape with a diameter of 3 mm; the holes have an area of 0.07 mm^2;
3. The teflon tape is rised and the wafer is placed under the hole in the tape;
4. The teflon tape is then attached to the sample with the help of a tool. When the teflon tape is rised again, the sample is rising as well this time;
5. The back of the wafer is scratched with a diamond pen, as it is not conductive and it should be removed to prevent insulation;
6. The back of the wafer is then scratched with a copper tool, in order to create a contact between the body of the electrode (copper sheet) and the wafer;
7. The copper sheet is placed below the wafer and the wafer is then located on it with the help of the teflon tape;

8. The teflon tape is attached to the copper and the extra tape is cut out;

9. A second layer of teflon tape should be added on top of the first, in order to prevent contamination of the sample.

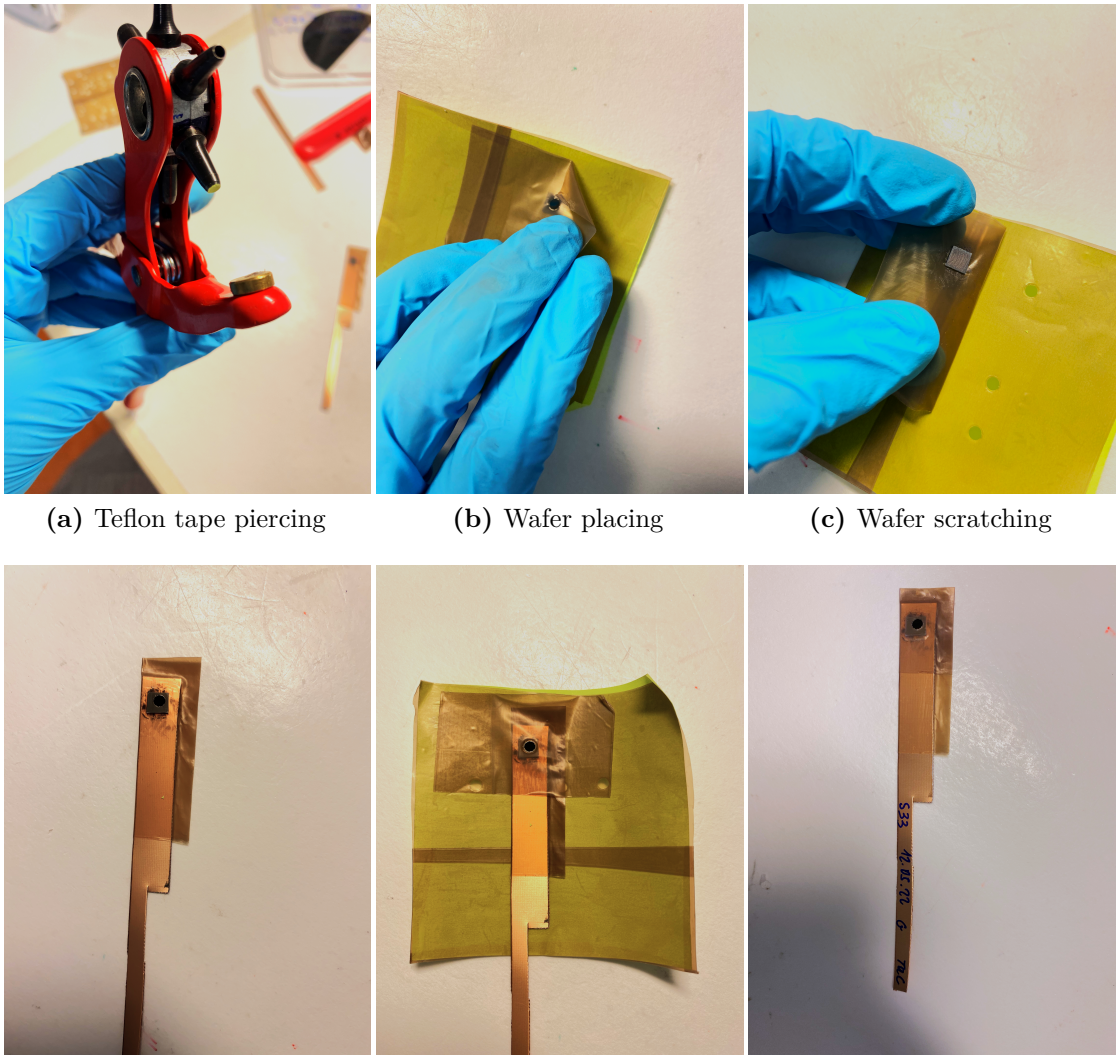

(a) Teflon tape piercing **(b)** Wafer placing **(c)** Wafer scratching

(d) First teflon layer **(e)** Second teflon layer **(f)** Final electrode

Figure 3.2: Electrode preparation procedure

3.6 Experimental setup

The electrochemical reactions are taking place in an electrochemical cell and they consist of two independent reactions at the working and counter electrodes. An electrolyte stands between the working and current electrodes, which allows charge transport thanks to an anionic current. The electrodes are connected to a potentiostat used to both measure and apply the potential to the system.

The focus of the work is the working electrode, therefore CV studies are used to measure the current flowing through the working electrode as a function of the applied potential thanks to the potentiostat. The reaction occurring at the counter electrode is opposite to that on the working electrode, in order to balance the redox reaction.

Different setups are shown in figures 3.3, 3.4 and 3.5. Table 3.1 summarizes the reference electrodes used in different setups. The first setup is used for measurements in plain PBS or for the washing step (DA removal from the imprinting sites). The second one is makes use of a connection for the reference electrode and it used for measurements in DA or AA. These analytes could cause damaging of the Ag/AgCl reference electrode, which needs therefore to be kept away from the solution. In this cases the connection is previously filled with PBS to ensure the connection. The last setup is used for the imprinting and it exploits a silver wire as a reference electrode. This is done as the solution contains pyrrole, which would easily damage the delicate Ag/AgCl electrode.

Use	**Reference electrode**
Measurements in PBS or washing	Ag/AgCl
Measurements in DA or other analytes	Ag/AgCl with PBS connection
Molecular imprinting	Ag wire

Table 3.1: Reference electrodes used in different setups

3.7 Modified electrode fabrication

The electrode modification is carried out by means of molecular imprinting technique, using DA as a target molecule and PPy as a conducting polymer. At first the imprinting solution containing the template molecule (DA) and the functional monomer (pyrrole) has to be prepared. As discussed in section 1.3, pyrrole has a partially cross-linking behaviour preventing the need for a cross-linker in the imprinting solution. The optimized ratio of DA and pyrrole is dissolved into previously nitrogen-purged and fresh PBS. The optimized parameters for the imprinting

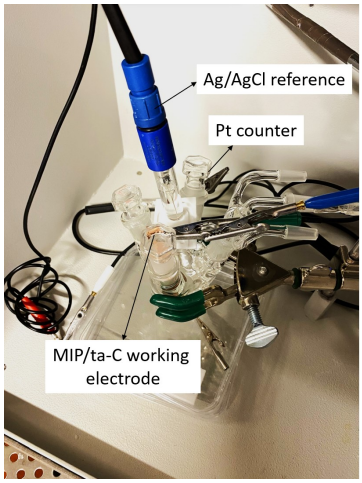

Figure 3.3: Experimental setup used for experiments in plain PBS (e.g. washing step)

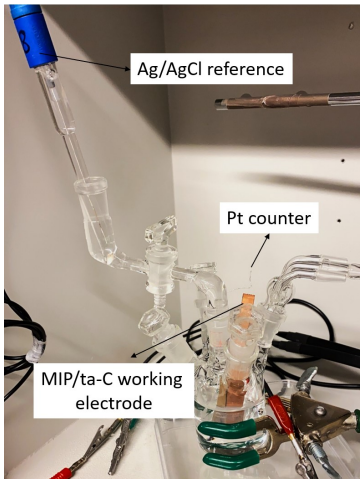

Figure 3.4: Experimental setup used for experiment in DA solutions

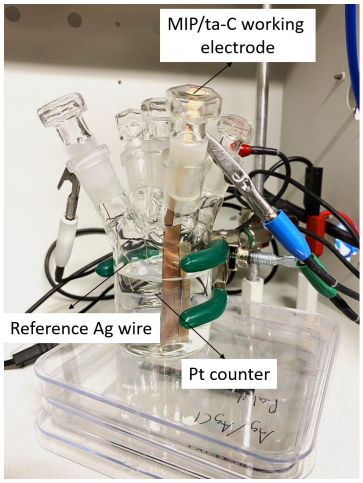

Figure 3.5: Experimental setup for the ta-C working electrodes DA imprinting

solution (ratio of DA and pyrrole and pH of the PBS used for the imprinting solution) are described in section 4.1.

The molecular imprinting of the working electrode is carried out electrochemically by means of a three-electrode system, as those shown in section 3.6. The system includes reference, counter and working electrodes. The electrodes involved in the process are a platinum counter electrode, a silver wire reference electrode and the working electrode previously discussed (section 3.5).

The ta-C electrode is placed into the freshly prepared and degassed 10x PBS solution (pH 8.0) containing 2.0 mM pyrrole and 2.0 mM DA, reaching a molar ratio of 1:1. The solution is placed into a voltammetric cell together with the three-electrode system: it is important for the electrodes not to be touching each other to prevent undesired connections. The CV method was employed for for the electro-polymerization of the MIP on the ta-C surface with scan rate of 100 mV/s in the potential range -0.2 to 0.8. The number of cycles carried out was 10. The optimized parameters are discussed in section 4.1. As the cycles of CV are carried out, a layer of PPy is polymerized onto the working electrode's surface. Figure 3.6 shows the current evolution of the cyclic voltammogram cycle after cycle. The current is decreasing every cycle, proving that the working electrode is now covered by a thicker PPy layer every cycle. It is important to point out that the PPy is containing DA molecules, which were provided into the imprinting solution.

The washing of the electrodes consists of two steps and it is meant to remove the DA molecules from the imprinting sites. The first step involves the placing

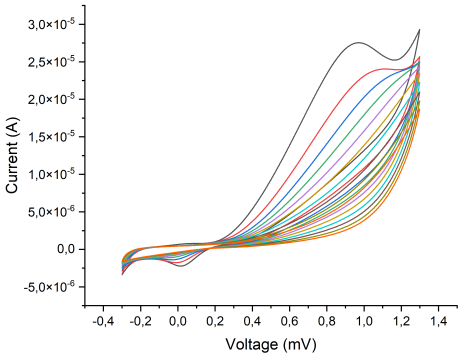

Figure 3.6: Imprinting step conducted by CV

of the electrodes into a solution of ethanol and DIW (50% of both). This step is meant to remove the unreacted monomers and DA from the electrode surface. The second step is the electrochemical template removal from the electrodes and it is performed by CV. A variable number of CV cycles (usually around 30) is carried out at high scan rate (usually 400 mV/s, so that the DA molecules can be extracted from PPy. After the CV, DPV is exploited as a more sensitive technique to make sure there is no peak for DA (around its oxidation potential) and therefore that it has been washed away.

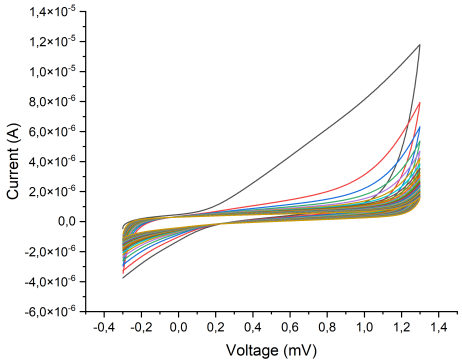

Figure 3.7: Washing step conducted by CV

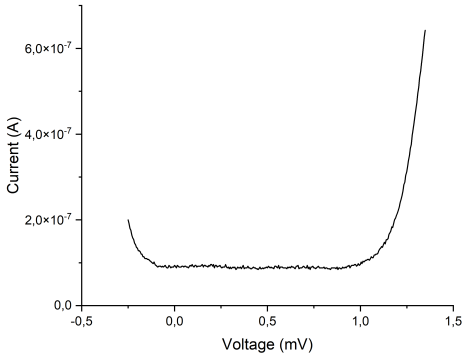

Figure 3.8: DPV study to check the DA peak is not present

3.8 Voltammetric DA detection

First, the DA solution of the required molarity is prepared. The optimization studies were carried out in 100 μM DA solutions in order to have higher oxidation currents to analyse, all the other studies were performed in 10 μM, which is the approximated DA concentration in physiological media and still provided good oxidation peaks.

After that, the working electrode was incubated into the solution for 10 minutes, which was found to be the best incubation time from the incubation study discussed in section 4.1.

After the incubation, a CV was performed with the following parameters:

- Scan rate: 300 mV/s
- Cycles: 2
- Initial potential: $-0.3\,mV$
- Final potential: $0.9\,mV$
- Maximum current: $0.016\,mA$
- Step size: $2\,mV$

Chapter 4

Results and discussion

4.1 Optimization of the experimental conditions

In order to enhance the behaviour of the electrochemical sensor designed, the experimental conditions were optimized. The parameters considered involved the imprinting solution and the detection process. Several parameters characterizing the imprinting solution were analysed: its pH, the molar ratio of target template molecule to functional monomer, the scan rate of the CV during the electrochemical polymerization and the thickness of the polymeric layer. After that, the scan rate of the CV for DA determination into the PBS solution was considered. At last, the incubation time was taken into account.

4.1.1 pH of the imprinting solution

The pH of the PBS solution used to prepare the imprinting solution was studied first. The imprinting solutions were prepared with constant parameters, apart from the pH of the PBS solution utilized, which are discussed in table 4.1.

The molar ratio of DA to pyrrole was chosen based on previous works on CNFs and it was considered to be 1:5, namely $0.0189\,g$ of DA ($2\,mM$) and $35\,\mu L$ of pyrrole ($10\,mM$). The electropolymerization of pyrrole was carried out electrochemically, as discussed above. The parameters used in the CV were once again based on previous studies; the scan rate was considered to be 100 mV/s and the number of cycles used was 10. The parameters were set to the below discussed values until they were optimized.

The optimization was carried out evaluating the performance of the imprinted electrode as the pH of the imprinting solution was varied. In particular, the electrodes were imprinted with the previously discussed parameters, washed and tested into a 100 μM DA solution in $0.1\,M$ PBS with pH 7.4 (physiological pH). The oxidation and reduction currents were evaluated and the pH showing the

Parameters	Value used
ratio DA : pyrrole	1:5 (2 mM : 10 mM)
CV cycles	10
CV scan rate	100 mV/s

Table 4.1: Parameters used for the imprinting of the working electrodes in the pH optimization

highest mean oxidation current was chosen. A higher current is in fact proving a better ability of the electrode to detect DA when the the concentration in the solution is kept constant.

The different pH values (3, 6, 7, 8, 9) analysed and the correspondent mean oxidation peak current are shown in figure 4.1.

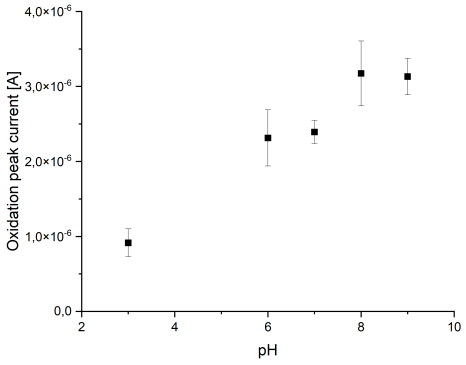

Figure 4.1: pH of the imprinting solution optimization

From the results presented it is clear that the best peak oxidation current was obtained when pH of the imprinting solution was 8. This result has been therefore fixed for the next steps in the optimization.

4.1.2 Ratio of DA and pyrrole concentrations in the imprinting solution

The effect of the molar ratio of functional monomer (pyrrole) to template molecules (DA as target analyte) in the imprinting solution on the oxidation peak current was then analysed.

The parameters for the imprinting are described in table 4.2 and, as mentioned in section 4.1.1, the pH has been fixed to 8 from this study on.

Parameters	Value used
pH	8
CV cycles	10
CV scan rate	100 mV/s

Table 4.2: Parameters used for the imprinting of the working electrodes in the ratio optimization

Once again, the imprinting solution was prepared and the electrodes were imprinted with the previously discussed CV parameters. After that, they were washed from the DA and tested in a 100 μM DA solution in 0.1 M PBS with pH 7.4 by means of CV. The molar ratios of DA to pyrrole taken into account are shown in table 4.3.

Ratio	DA	Pyrrole
1:1 (2 mM : 2 mM)	0.0189 g	7 μL
1:3 (2 mM : 6 mM)	0.0189 g	21 μL
1:5 (2 mM : 10 mM)	0.0189 g	35 μL
1:7 (2 mM : 14 mM)	0.0189 g	49 μL
1:9 (2 mM : 18 mM)	0.0189 g	63 μL

Table 4.3: Ratio of the concentration of DA and pyrrole utilized for the preparation of the imprinting solutions

The mean peak oxidation currents were measured in the 100 μM DA solution in 0.1 M PBS with pH 7.4 and compared, as shown in figure 4.2.

From the presented result it can be found that the best ratio for the imprinting solution is 1:1. As a result, this ratio has been applied for the next studies.

As the amount of pyrrole in the solution increases, the DA becomes the limiting reagent in the reaction. Since the DA molecules are too few, they remain trapped in the deeper PPy layers, leading to a decrease in the number of imprinted sites and an overall worse performance of the electrode. As discussed in the section 4.3, PPy is characterized by a lower conductivity with respect to ta-C, causing a weaker interaction between the electrode and the analyte. The recognition sites function as receptors or artificial antibodies and they are in fact acting as "gates" through the PPy layer for the DA molecules, allowing the current flow through the electrode. As a consequence, the increase in the pyrrole and, as a result, the reduction of the recognition sites leads to the lowering of the current flow in the electrode and to a worsening of the performance of the sensing system.

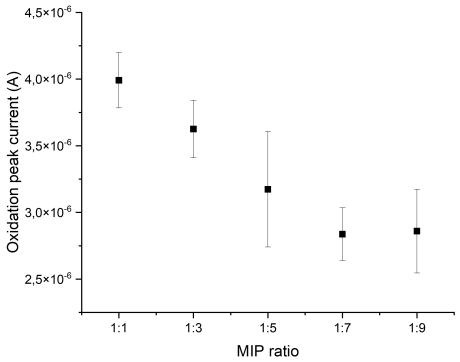

Figure 4.2: Optimization of the ratio between DA and pyrrole concentrations in the imprinting solution

4.1.3 Number of CV cycles for electropolymerization and thickness of the MIP layer

The effect of the MIP layer thickness was then analysed to improve the performance of the ta-C/MIP toward DA detection. As already discussed, the MIP layer is formed by electropolymerization and the number of CV cycles used determines the thickness of the polymeric coating. The numbers of cycles taken into account are listed in the following: 5, 10, 15, 20.

Once again, electrodes were prepared and modified by electrochemical molecular imprinting, then washed electrochemically by means of CV in PBS and tested in a 100 μM DA solution in 0.1 M PBS with pH 7.4. The parameters used in the imprinting solution and electropolymerization are described in table 4.4.

Parameters	**Value used**
pH	8
Molar ratio	1:1
CV scan rate	100 mV/s

Table 4.4: Parameters used for the imprinting of the working electrodes in the ratio optimization

The mean peak oxidation currents were computed for each thickness of the MIP layer and they are reported in figure 4.3

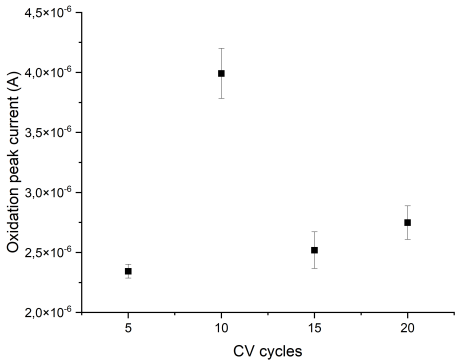

Figure 4.3: Optimization of the CV cycles (thickness of the MIP layer) required for the imprinting of the electrodes

As it is clear from figure 4.3, the optimal thickness for DA sensing is given by 10 CV cycles and it is used in the next experiments.

As the thickness of the MIP layer increases, a larger number of recognition sites is formed and the current increases. After 10 cycles, the higher thickness does not help the recognition anymore, as the template molecules remain trapped in the PPy layer being harder to remove from their sites and making the binding of the target more difficult. Due to the lower amount of available recognition sites, the response signal is decreased again. In addition, the template removal step for higher number of cycles is more complicated and time consuming.

4.1.4 Scan rate of the CV for electropolymerization

The scan rate of the CV electropolymerization was then analysed and optimized. Once again, the already optimized parameters were updated, leading to those discussed in table 4.5.

Parameters	Value used
pH	8
Molar ratio	1:1
CV cycles	10

Table 4.5: Parameters used for the imprinting of the working electrodes in the CV scan rate optimization

The electrodes were imprinted, washed and tested as in the other optimization

steps with the discussed parameters. The scan rate used in the electrochemical imprinting of the electrodes was varied considering the following values: $10\,mV/s$, $50\,mV/s$, $100\,mV/s$, $150\,mV/s$ and $200\,mV/s$. The oxidation mean currents were analysed and reported in figure 4.4.

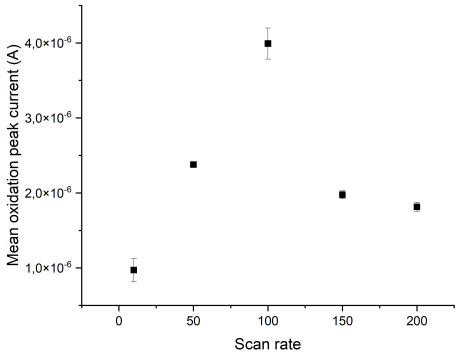

Figure 4.4: Optimization of the CV scan rate required for the imprinting of the electrodes

Figure 4.4 shows that the scan rate of $100\,mV/s$ was definitely the best among the ones analysed. This values is then adopted in the following studies.

A lower potential scan rate could in fact form a tighter film, decreasing the number of imprinted sites available. On the other hand, a higher scan rate might form a looser film, making recognition capacity worse once again. As a consequence, the best scan rate was found to be $100\,mV/s$, as it maximizes the performance of the PPy for the imprinting.

4.1.5 Incubation time in the DA solution

At last, the incubation time in the $10\,\mu M$ DA solution in $0.1\,M$ PBS with pH 7.4 was investigated. The electrodes were first imprinted with the optimized parameters shown in table 4.6, then washed and tested in a $10\,\mu M$ DA solution in $0.1\,M$ PBS with pH 7.4.

Parameters	Value used
pH	8
Molar ratio	1:1
CV cycles	10
CV scan rate	100 mV/s

Table 4.6: Parameters used for the imprinting of the working electrodes in the incubation time optimization

Before the electrodes were tested, they were left incubating for a certain time inside the same $10\,\mu M$ DA solution used for testing. The incubation time has been varied considering the following values: 0 minutes, 1 minute, 5 minutes, 10 minutes, 15 minutes and 20 minutes. The oxidation peak mean current has been then measured for each incubation time value and it is shown in figure 4.5.

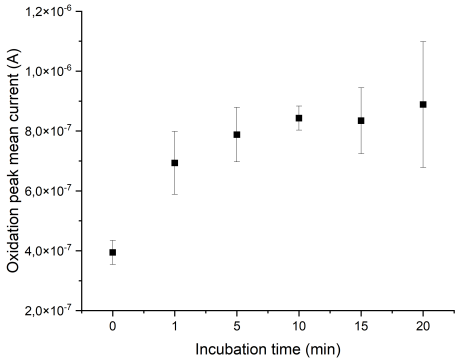

Figure 4.5: Optimization of the incubation time inside the testing solution

The incubation grants the DA molecules the time to diffuse through the solution in order to reach the recognition sites and occupy them. As shown in figure 4.5, the current saturates for high enough incubation time (10 minutes) leaving the response signal basically unchanged. This implies the DA molecules have had the time to diffuse through the solution to the recognition sites, which are then completely occupied. The 10-minute incubation time was applied to the next studies for DA pre-adsorption, as after that time the response current is constant. This incubation time is chosen as a matter a convenience, as it allows the shortest time to result. Thanks to this trick, a lower concentration of DA could be detected making the sensor more sensitive.

The advantageous effect of the incubation can be confirmed by figure 4.6, which

shows the CV carried out without any incubation and after a 10-minute incubation time.

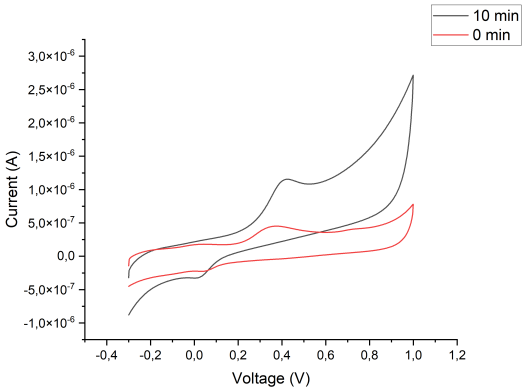

Figure 4.6: Effect of the incubation on the electrode performance

Figure 4.6 points out the effect of the incubation on electrode's performance. The mean oxidation current has been computed and it was found to be more than doubled when a 10-minute incubation was applied on DA-imprinted electrodes. In particular, the mean oxidation current without incubation was $3.94 \cdot 10^{-7}\,A$ while the one found after the 10-minute incubation period was $8.43 \cdot 10^{-7}\,A$.

4.2 Physical characterization

4.2.1 Scanning electron microscopy (SEM)

SEM is often used to obtain the surface morphology of the samples under investigation. Its working principle is based on the scanning of a focused electron beam on the surface of the specimen in vacuum. Several detectors are exploited, considering backscattered electrons, secondary electrons and more. It is important to point out that the samples need to be conductive to prevent surface charging. The ta-C and MIP/ta-C samples were sufficiently conductive not to require surface coating, although a low acceleration potential was chosen [44].

Different ta-C and MIP/ta-C samples were analysed by means of SEM in order to study the surface morphology of ta-C and MIP/ta-C electrodes. Both front and cross sectional images of the samples were taken into account in order to show the surface morphology and the different layers of the samples. The results are discussed below.

Figures 4.7 and 4.8 show front SEM images of plain ta-C samples with magnifications respectively of $10k\,X$ and $25k\,X$. In both cases it is clear that the morphology

of the sample is flat and there are no significant changes across the whole sample.

Front images were taken for MIP/ta-C samples as well in order to allow a comparison between the two samples. The MIP/ta-C samples were carefully washed with ethanol and dried to remove the presence of salts on the surface. It is clear that the surface modification has been carried out, even though the molecularly imprinted recognition sites are too small to be seen at the SEM.

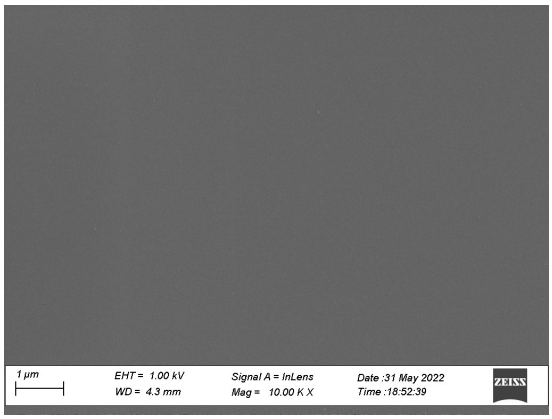

Figure 4.7: Front SEM images of a ta-C sample with magnification 10k X

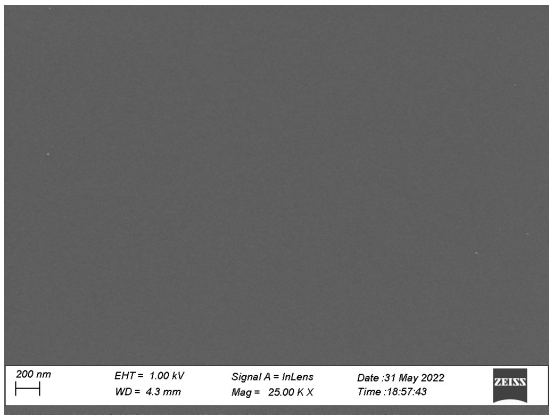

Figure 4.8: Front SEM images of a ta-C sample with magnification 25k X

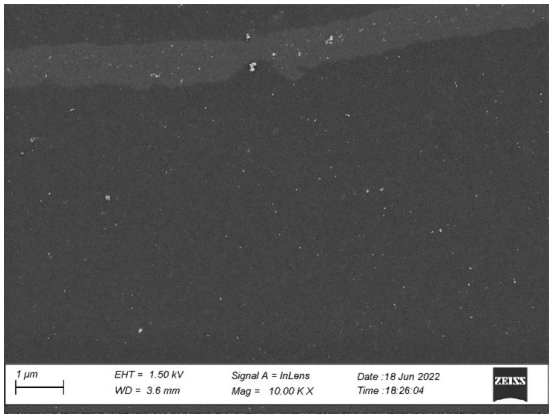

Figure 4.9: Front SEM images of a MIP/ta-C sample with magnification 10k X

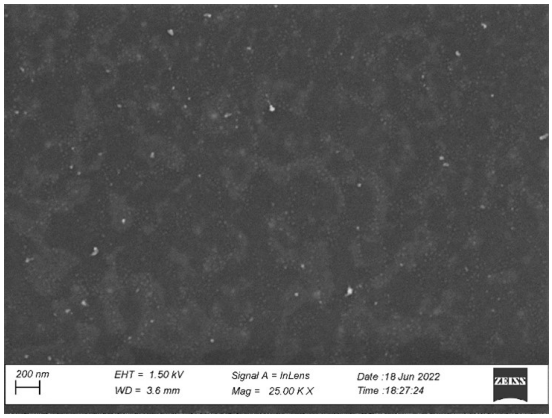

Figure 4.10: Front SEM images of a MIP/ta-C sample with magnification 25k X

Cross sectional SEM images of the different samples were taken into account. The samples analysed are the same considered in the study discussed in section 4.6.

All the images presented (4.11, 4.12, 4.13) show the ta-C layer on top of the silicon. Figure 4.13 shows a brighter region, which represents the titanium adhesion layer.

Unfortunately, the PPy layer is too thin to be seen by SEM images, leading to very similar images for the ta-C sample and the MIP/ta-C one.

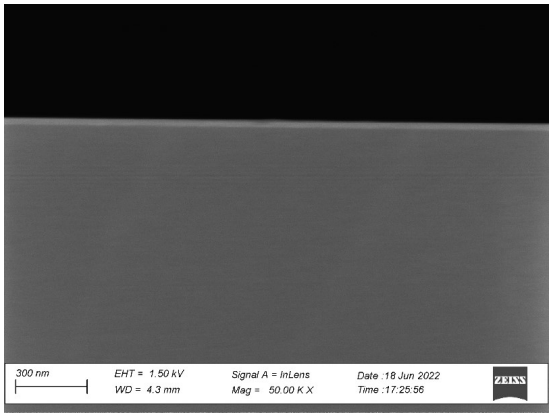

Figure 4.11: Cross sectional SEM images of a ta-C sample

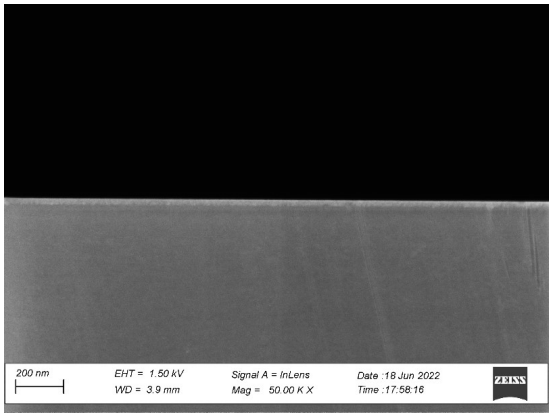

Figure 4.12: Cross sectional SEM images of a MIP/ta-C sample

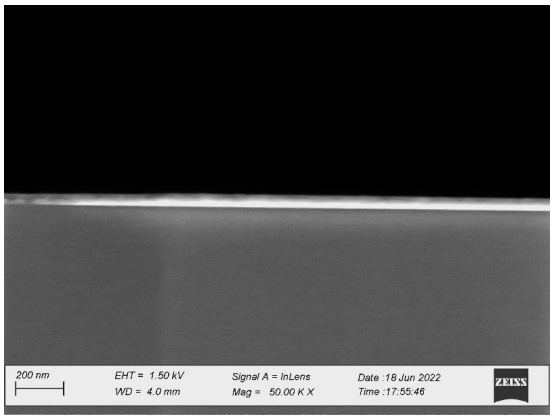

Figure 4.13: Cross sectional SEM images of a ta-C sample with titanium adhesion layer

4.2.2 Raman spectroscopy

Raman spectroscopy is used to study the bonding structure of the ta-C and MIP/ta-C films. This method is based on the shining of a monochromatic laser beam on the sample, which interacts with the molecules and causes an energy shift in the collected signal [44].

The Raman spectroscopy was carried out by means of a Micro-Raman spectroscope (WITech Alpha 300 RA6) equipped with an optical microscope. The laser excitation wavelegnth used for the measurements was $532\,nm$ using a $50X$ objective lens. Line scanning was performed using a $3\,mm$ line length containing 50 points (10 accumulations per point) and $0.5\,s$ integration time.

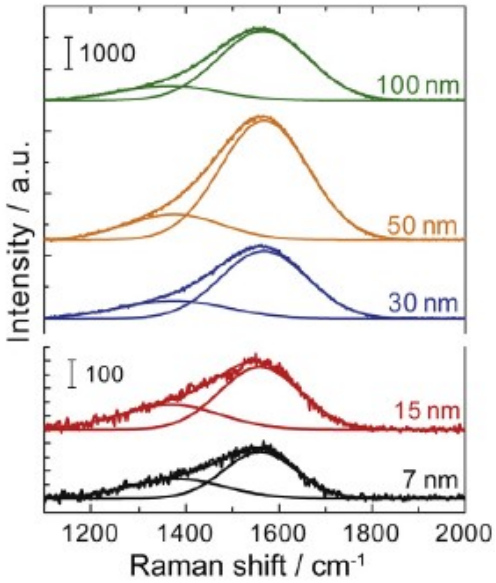

Figure 4.14: Raman spectrum for ta-C samples with different thickness [45]

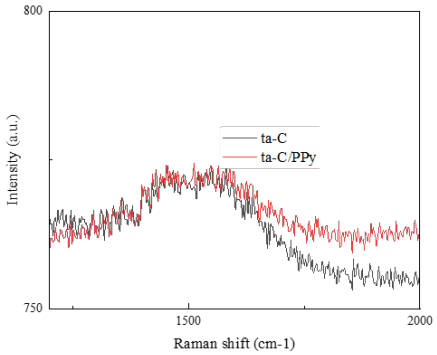

Figure 4.15: Raman spectrum of a 15 nm ta-C sample compared to an MIP-modified 15 nm ta-C sample

The Raman spectra in figure 4.14 already considered in previous research show a D band around $1360\,cm^{-1}$ and a G band around $1550\,cm^{-1}$. The mentioned peaks are related to the sp^2 fraction in the ta-C films, which decreases for higher thickness of the film [45]. Figure 4.14 shows the changing in the Raman spectrum for different thickness of the ta-C layer.

The Raman study was repeated for a MIP-modified $15\,nm$ ta-C sample, as shown in figure 4.15. Unfortunately, it was not possible to spot the presence of the PPy layer in the Raman spectrum. This might be related to the fact that the PPy

layer is extremely thin, as proved by the SEM study, leading to a difficulty in the appereance of a related peak in the Raman spectrum.

4.2.3 Atomic force microscopy (AFM)

The root mean square (RMS) roughness (R_q) was evaluted by means of a Bruker Dimension Icon AFM. After acquisition, the images were processed using Gwyddion 2.47 software for artifact correction and calculation or the R_q. The ta-C and MIP/ta-C samples have been analysed by means of AFM and surface topography maps have been obtained for them both.

Table 4.7 shows the roughness computed for both MIP-modified and unmodified silicon and ta-C samples. The roughness was evaluated in a $5x5\,\mu m$ square on the surface of the different samples. This surface area was chosen in order to guarantee the analysis of a larger portion of the sample, as its surface morphology might vary. The 3D roughness maps collected on the different samples are shown in figures 4.16, 4.17 for the silicon samples and in figure 4.18 and 4.19 for the ta-C samples. The AFM study has been carried out on a silicon sample as well in order to evaluate the actual effect of MIP on a substrate.

Table 4.7 shows the roughness on the different samples analysed. It is clear that the MIP modification brings about a significant increase of the surface roughness. This implies a better binding performance toward the DA molecules thanks to the higher surface area available. The formation of the DA-imprinted sites can be considered the reason why the roughness has increased. Last, this is proof that the surface modification has occurred.

	ta-C	**MIP/ta-C**	**Si**	**MIP/Si**
R_q **[nm]**	0.783	1.11	0.351	1.38

Table 4.7: RMS surface roughness values obtained in the AFM sudies of plain ta-C, MIP/ta-C, plain silicon and MIP/Si samples in $5\,\mu m\,X\,5\,\mu m$ region on the sample

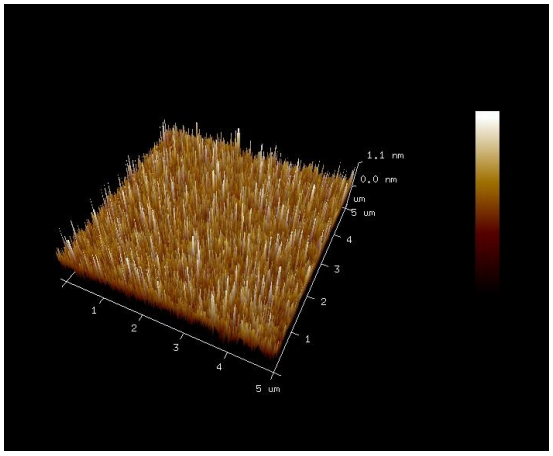

Figure 4.16: AFM 3D surface topography map of a bare silicon sample

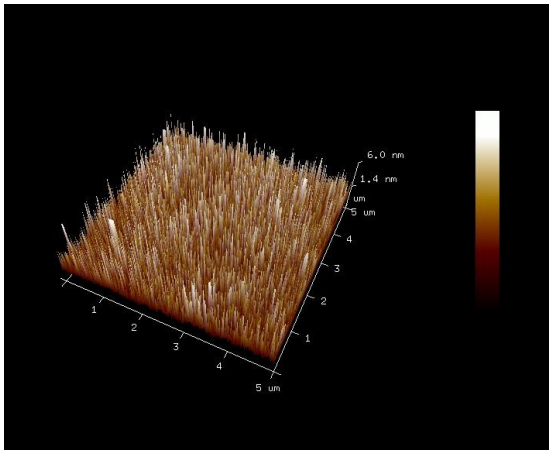

Figure 4.17: AFM 3D surface topography map of a MIP-modified silicon sample

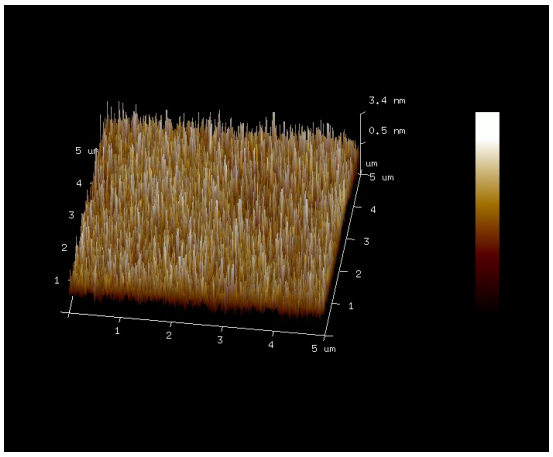

Figure 4.18: AFM surface topography map of a ta-C sample

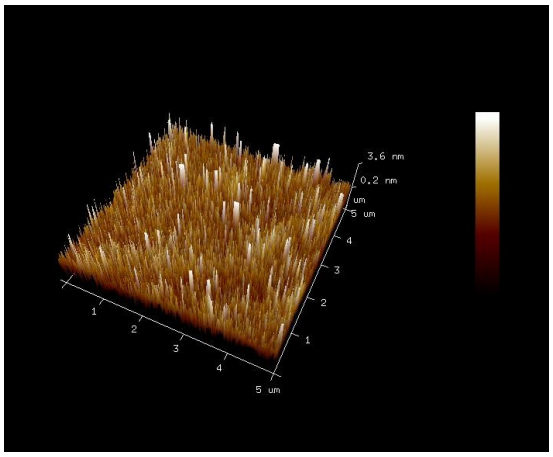

Figure 4.19: AFM surface topography map of a MIP/ta-C sample

4.3 Electrochemical characterization

Two different redox probes were used for the characterization of the MIP/ta-C electrodes under investigation. One was an inner-sphere redox (ISR) probe, DA, and the other an outer-sphere redox (OSR) probe, hexaammineruthenium ($Ru(NH_3)_6^{3+}$).

The latter is characterized by a positive charge. Th OSR probes are considered to be insensitive to the surface chemical properties, although they can provide information on the electronic properties of the electrode material. Differently, ISR probes are highly sensitive to surface chemistry and their oxidation requires specific interaction between them and the surface [46, 44]. It is important to point out that in this study DA is used as a template molecule in the molecular imprinting process and as a probe.

4.3.1 Testing in hexaammineruthenium (OSR)

Unmodified ta-C, MIP and NIP electrodes were tested in a $5\,mM\ Ru(NH_3)_6^{3+}$ solution in $0.1\,M$ KCl using CV technique.

Figure 4.20 shows the behaviour of different electrode types in the previously discussed ruthenium solution. It is clear that the best redox signals are shown by the unmodified ta-C electrode. MIP/ta-C and NIP/ta-C electrodes are less conductive as the ta-C layer is covered by the PPy coating, which increases the resistance of the sample. MIP/ta-C electrodes show a better current response when compared to NIP/ta-C ones due to the recognition sites in the PPy coating created during the DA removal. In these regions, electrons can directly flow through ta-C, increasing the response current.

The same electrodes were tested for EIS in the same solution, leading to the result shown in figure 4.21.

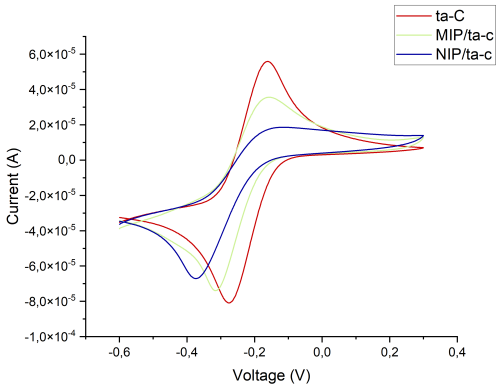

Figure 4.20: Electrochemical characterization in 5 $mM\ Ru(NH_3)_6^{3+}$ solution in 0.1 M KCl

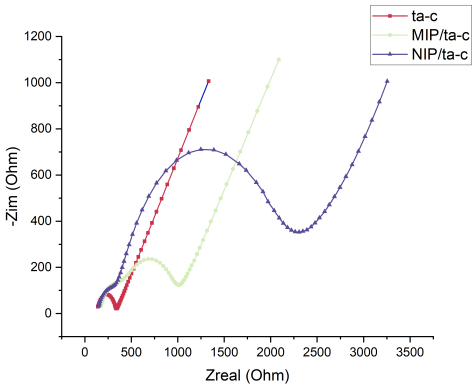

Figure 4.21: Nyquist plots of the EIS study in 5 $mM\ Ru(NH_3)_6^{3+}$ solution in 0.1 M KCl

Table 4.8 shows the data extracted from the EIS study after the fitting of the

curves to a modified Randles equivalent circuit shown in figure 4.22. The circuit shown is made of a resistance R_s, namely the solution resistance, in series with a parallel circuit with the charge transfer resistance R_{ct}, a Warburg element W and a constant phase element CPE in place of the double layer capacitance (C_{dl}). In this model, R_{ct} represents two different resistances: the electron transfer to the electrode surface and the electron transport through the film [45].

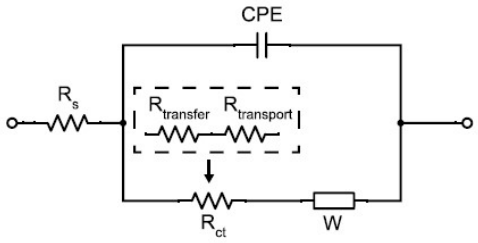

Figure 4.22: Randles equivalent circuit used to fit the Nyquist plots of the samples [45]

The curves were fitted through the Levenberg-Marquardt method, by means of a model including diffusion. The EIS studies analyse the signal as a function of the frequency, while the potential is kept constant. EIS can be used to study interfacial processes, such as redox reactions at electrodes [47]. The impedance spectra are usually made of a semi-circle and a linear region. The semi-circle is related to the the coupling of charge transfer resistance with the double layer capacitance at high frequency, while the straight line refers to the mass transfer impedance at low frequencies [47]. The straight line is related to the diffusion process, while the diameter of the semicircle describes the electron transfer resistance (R_p). Figure 4.21 and table 4.8 show how the R_p is increased after the NIP or MIP modification of the electrode. This is due to the presence of less-conductive PPy film, which introduces resistance at the interface between the electrode and the solution. The MIP modification is characterized by a lower resistance when compared to the NIP, as the recognition sites provide a gate for the electrons, improving the electron transfer. On the other hand, the R_u represents the solution resistance and it corresponds to the first point of the semicircle in the lower impedance region. This is expected to be constant for all the electrodes analysed, as the solution used was always the same. At last, k^0 is the apparent heterogeneous rate constant and it is inversely proportional to the charge transfer resistance. It is indeed a measure of the kinetics of a redox couple, expressing the velocity needed for the system to reach the equilibrium state. A higher k^0 value represents a faster achievement of the equilibrium, while a lower one would represent a slower process. The heterogeneous rate constant is an important electrochemical parameter to compare electrode

materials [44].

This parameter can be computed considering the following equation:

$$k^0_{app} = \frac{RT}{F^2 A R_{ct}(c^b_o)(c^b_R)^{1-\alpha}} \tag{4.1}$$

where R is the gas constant, T the temperature, F the Faraday's constant, A the geometrical area of the electrode, c the concentration and α the transfer coefficient. The subscripts O and R refer to the oxidized and reduced species, while the subscript b denotes the bulk concentration [45]. The obtained values are consistent with the discussion carried out above, as their lower value is for the NIP and they increase to a maximum value for the ta-C sample. This underlines how the charge transfer resistance is higher in the case of NIP and lower for the plain ta-C sample. The double semicircle shown in the MIP/ta-C and NIP/ta-C curves is due to a double process occurring in the reaction under investigation. This suggests an electroactive behaviour of the PPy film, which has also been proved in studies such as [48]. The redox reaction causes a change in the electrical properties of the film from an insulator to a conductor involving electron and ion transport within the film [48].

Table 4.8 reports the data obtained from the analysis of the EIS studies in the OSR probe, while table 4.9 refers to the CV study.

The value of I_{pa}/I_{pc} gives insights about the reversibility of the redox process. The process is considered to be reversible for the ta-C substrate, as the value of this parameter is very close to 1. Differently, the process is considered to be irreversible for the NIP/ta-C and MIP/ta-C samples, as the current ratio is much higher than 1.

Sample type	**Ru [ohm]**	**Rp [ohm]**	k_0 **[cm/s]**
ta-C	130.7	198.4	0.0378
NIP/ta-C	130.0	$2.3 \cdot 10^3$	0.0033
MIP/ta-C	132.2	921.4	0.0081

Table 4.8: Data extracted from the EIS study

Sample	**Ipa [A]**	**Ipc [A]**	**Ipa/Ipc**	**Epa [mV]**	**Epc [mV]**	**ΔEp [mV]**	**Eon [mV]**
ta-C	$7.34 \cdot 10^{-5}$	$-8.23 \cdot 10^{-5}$	1.12	-161.9	-275.7	113.8	-274.9
NIP/ta-C	$3.11 \cdot 10^{-5}$	$-6.43 \cdot 10^{-5}$	2.07	-114.0	-373.7	259.7	-312.2
MIP/ta-C	$4.40 \cdot 10^{-5}$	$-7.45 \cdot 10^{-5}$	1.69	-156.1	-315.9	159.8	-287.6

Table 4.9: Data extracted from the CV in hexaammineruthenium (OSR) for different samples

4.3.2 Testing in DA

A further study in DA was meant to electrochemically characterize the electrodes under analysis. As mentioned above, DA is an ISR probe and it is subjected to both chemical and electrochemical reactions on electrode materials. At the same time, it is the template molecule of the MIP and the target of the sensor. This implies this study aims to prove how the ta-C/MIP sensor enhances the DA recognition, leading to a higher sensitivity.

Looking at figure 4.23, it is clear that there is a significant advantage in using MIP/ta-C electrode when compared to unmodified ta-C ones. The current response is indeed increased leading to a higher sensitivity for DA. In addition, MIP/ta-C electrodes are also characterized by a better performance with respect to NIP electrodes, which in turn detect DA better than unmodified ta-C electrodes. The same has been proved in the study discussed in section 4.6. The ΔE_p has been calculated for this CV study as well and the results are showed in table 4.10. Once again, the values found are sufficiently distant from the value of $29.5\,mV$ to define the reaction irreversible.

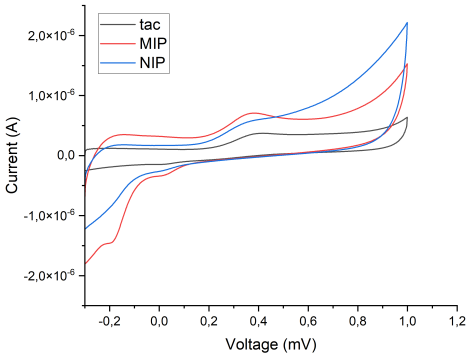

Figure 4.23: Electrochemical characterization in 10 μM DA solution in 1X PBS 7.4

Sample type	ΔEp [mV]
ta-C	202
NIP	193
MIP	192

Table 4.10: ΔE_p computed for different samples

4.4 Effect of the scan rate on the DA detection

The effect of the CV scan rate in the testing of the MIP/ta-C electrodes in DA has been addressed in order to understand the detection mechanism of the sensing system. The electrodes were imprinted with the techniques discussed in the previous sections and using the optimized parameters. After they were washed and the template molecule had been removed, they were tested in a $10\,\mu M$ DA solution in PBS (physiological pH 7.4).

The potential scan rates taken into account for this study are listed in the following: $10\,mV/s$, $20\,mV/s$, $100\,mV/s$, $200\,mV/s$, $300\,mV/s$.

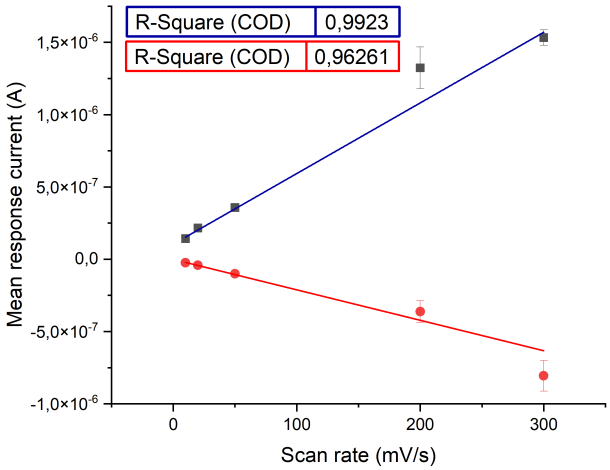

Figure 4.24: Mean oxidation and reduction currents as a function of the CV potential scan rate for 10 μM DA detection

The behaviour of the oxidation and reduction currents was studied and it was found that they have a linear dependence on the potential scan rate. As a result, figure 4.24 shows the mean oxidation and reduction currents for each recorded potential scan rate as a function of the scan rate potential.

The coefficient of determination (COD) R^2 describes how much the variation of the dependent variable can be predicted from the independent variable. It can be used to determine how well the line fits the given data. Tables 4.11 and 4.12 show the CODs for the fitting considering respectively the oxidation and reduction mean currents as a function of the potential scan rate and its square root, respectively. It is clear from the CODs that the oxidation mean current data is much better fitted by a linear curve when expressed as a function of the potential scan rate.

Oxidation mean current as a function of the potential scan rate COD	Oxidation mean current as a function of the square root of the potential scan rate COD
0.9923	0.9475

Table 4.11: Coefficient of determination R^2 for the linear fitting considering the oxidation mean current as a function of the potential scan rate and its square root, respectively

Reduction mean current as a function of the potential scan rate COD	Reduction mean current as a function of the square root of the potential scan rate COD
0.96261	0.74221

Table 4.12: Coefficient of determination R^2 for the linear fitting considering the reduction mean current as a function of the potential scan rate and its square root, respectively

This study has been carried out in order to better understand the electrode reaction kinetics and the interfacial behaviour of electroctive compounds. In particular, the goal was to determine whether the detection mechanism of the electrodes under analysis for DA is based on diffusion or adsorption. The detection mechanism is based on diffusion if species are freely diffusing in the solution, while adsorption occurs when species are already adsorbed on the electrode surface.

According to [49], adsorption and diffusion mechanisms are described by different equations, which are discussed below.

The one shown below is the Randles-Sevcik equation and it describes the dependence of the peak current on the potential scan rate for electrochemically reversible electron transfer processes which involve freely diffusing redox species. The same equation also explains that a plot of i_p versus $\nu^{1/2}$ should be linear [49].

$$i_p = 0.446nFAC^0\left(\frac{nF\nu D_0}{RT}\right)^{1/2} \tag{4.2}$$

In the following the parameters present in the Randles-Sevcik equation are described:

- i_p is the peak response current
- n is the number of electrons participating in the redox
- F is the Faraday's constant
- ν is the scan rate

- D_0 is the diffusion coefficient of the oxidized analyte
- A is the electrode surface area
- C^0 is the bulk concentration of the analyte
- R is the universal gas constant
- T is the temperature

Differently, for electrode-adsorbed species the current response is described by the following equation [49].

$$i_p = \frac{n^2 F^2}{4RT} \nu A \Gamma^* \tag{4.3}$$

In the previous equation Γ^* is the surface area coverage of the adsorbed species.

These two equations prove that the current response for adsorbed species is expected to vary linearly with the potential scan rate. Differently, for diffused species the response current will vary linear with its square root, as in the current case.

4.5 Effect of the DA concentration on the recognition

The MIP/ta-C electrodes were evaluated by DPV in various PBS (pH 7.4) solutions with different DA concentrations. This study was meant to determine the limit of detection of the electrodes, as well as their sensitivity. The concentrations taken into account are listed in the following: $25\,nM$, $50\,nM$, $100\,nM$, $250\,nM$, $500\,nM$, $750\,nM$, $1\,\mu M$.

The study was carried out starting from a DA concentration of $25\,nM$ and spiking the correct amount of solution from a mother solution to increase the concentration of DA.

Figure 4.25 shows the DPV plots for the some among the different DA concentrations tested. It is straighforward that the current peak becomes higher as the concentration is increased and it is easier for the electrode to detect the target analyte.

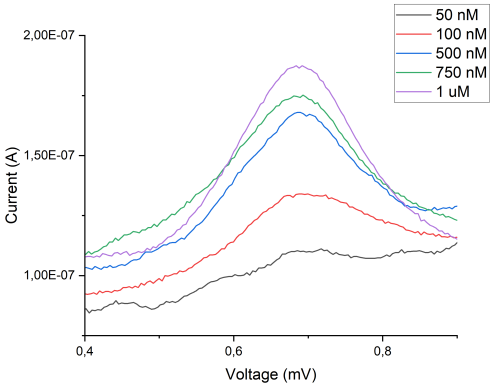

Figure 4.25: DPV curves for solutions with different DA concentrations in PBS with pH 7.4

Figure 4.26 shows the computed mean oxidation currents as a function of the DA concentration in the testing solution (in PBS 7.4). As shown by the linear fitting carried out, the data follows two different linear behaviours depending on the concentration range. Although only three points have been analysed, a first linear behaviour can be observed between $25\,nM$ and $100\,nM$ concentrations. This first linear fitting is characterized by a R^2 of 0.99986, highlighting the high linear dependence of the points. The second linear includes five points, leading to a more robust interpretation of the results. The second range has been found between $100\,nM$ and $1\,\mu M$ concentrations and it is characterized by an R^2 factor of 0.99526, which is also extremely high. Figure 4.27 shows a close-up of the second linear range, which is considered to be the main one.

The presence of two linear ranges ($25\,nM - 100\,nM$ and $100\,nM - 1\,\mu M$) could be due to the different affinity level and non-uniform distribution of recognition sites in the PPy film. For low DA concentration, the molecules tend to occupy high affinity recognition sites at the surface of the PPy coating. When these sites are occupied, molecules start to bind in the lower affinity sites, deeper in the PPy. As a result, the slope of the linear fitting curve is decreased [50].

The linear behaviour of the plots implies that the oxidation response current grows linearly with the concentration of the DA in the solution, namely the target analyte. The linear response in a certain linear range is extremely important as it allows to use the sensor to easily predict the concentration values in a real sample given the response signal.

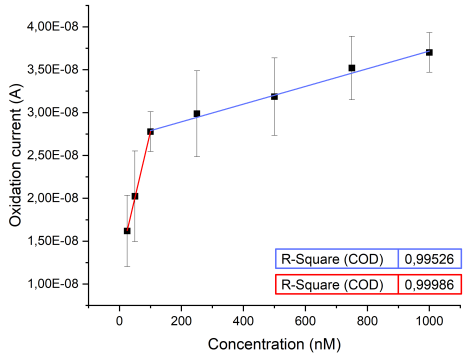

Figure 4.26: Mean oxidation peak current as a function of the concentration of DA in the testing solution and linear fitting

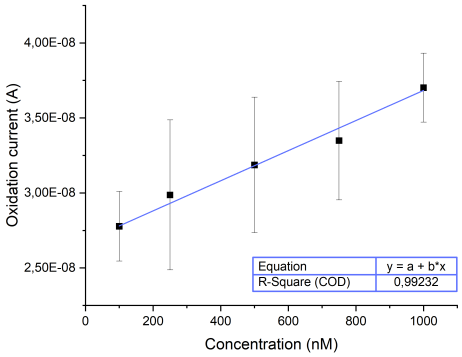

Figure 4.27: Close-up of the mean oxidation peak current as a function of the concentration of DA in the testing solution and linear fitting

The LOD and sensitivity (S) of the sensor have been computed considering the following formulas.

$$LOD = \frac{3 \cdot \delta}{m}; \quad S = \frac{10 \cdot \delta}{m} \tag{4.4}$$

In the previous equations δ corresponds to the standard deviation of the blank, while m represents the slope of the linear fitting.

The results of the calculations are reported in table 4.13. The slope used in the calculation refers to the linear fitting of the higher concentration range.

Parameter	**Value**
Sensitivity	S = 162 nM
Limit of detection	LOD = 48.6 nM

Table 4.13: Sensitivity and LOD of the MIP/ta-C sensor under study

It is important to point out that the sensitivity and LOD of the sensor were computed considering the least steep linear range (between 100 nM and 1 μM). This choice comes from the fact that the second linear range contains the most of the concentrations analysed and therefore allows a more robust fitting of the points. If the steepest curve had been considered for these calculations (between 25 nM and 100 nM), the LOD could become 3.53 nM, while the sensitivity could reach 11.8 nM.

Sainio et al. have studied the performance of $7\,nm$ unmodified ta-C with a $20\,nm$ titanium adhesion layer and the performance of the electrodes under analysis ($15\,nm$ MIP/ta-C without titanium adhesion layer) has been compared to their results. The previous work had found a sensitivity between $500\,nM$ and $1\,\mu M$ towards DA for the unmodified ta-C. This implies that the MIP/ta-C electrodes provide a significant improvement in the detection performance towards DA [51]. It has to be considered that ta-C behaves differently varying the thickness and depending on the presence of the titanium adhesion layer. In the study discussed in section 4.6, the $7\,nm$ ta-C sample with $20\,nm$ titanium adhesion layer has been found to be the best for unmodified ta-C samples among the samples analysed. Considering the poorer performance of the sample under study, molecular imprinting is found to be extremely helpful for the sensitivity of the sensor towards DA.

In conclusion, in order to evaluate the material's applicability for DA detection, it is important for the sensor to be able to detect a physiologically meaningful DA concentration. This concentration has been considered to be in the range $5 - 700\,nM$ for DA, proving the significancy of the current work [51].

4.6 Effect of the presence of a titanium adhesion layer in the sample and thickness of the ta-C

Different electrode materials were analysed in order to understand which of them provides the best results in the sensing of DA. The following materials were taken into account:

- 15 nm ta-C deposited on the silicon substrate
- 15 nm ta-C deposited on 20 nm titanium adhesion layer on the silicon substrate
- 7 nm ta-C deposited on 20 nm titanium adhesion layer on the silicon substrate

Figures 4.28 and 4.29 show schematics of the samples used and described above.

The effect of the presence of the titanium adhesion layer and thickness of the ta-C layer were studied testing the DA-imprinted electrodes in a $10\,\mu M$ DA solution in PBS with pH 7.4.

Figure 4.30 is meant to compare the performance of different electrode materials both MIP-modified and unmodified. It is clear that the MIP improves the performance of the detection, as the response current is higher for the MIP-modified electrodes when compared to the unmodified case. Furthermore, different sample materials provide different performances that are discussed in the following.

Let us first focus on the unmodified ta-C showed in orange colour in figure 4.30 and whose CV curves are shown in figures 4.31 and 4.32.

The thickness of the ta-C layer affects the conduction of the current through the sample. The response current is indeed higher for a thinner ta-C coating, as

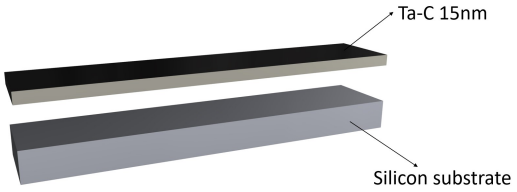

Figure 4.28: Schematic of a ta-C sample without titanium adhesion layer

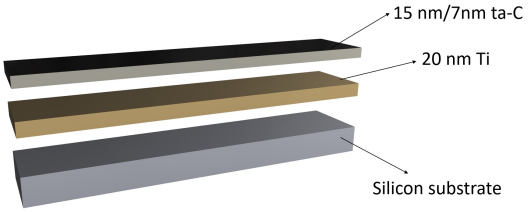

Figure 4.29: Schematic of a ta-C sample with titanium adhesion layer

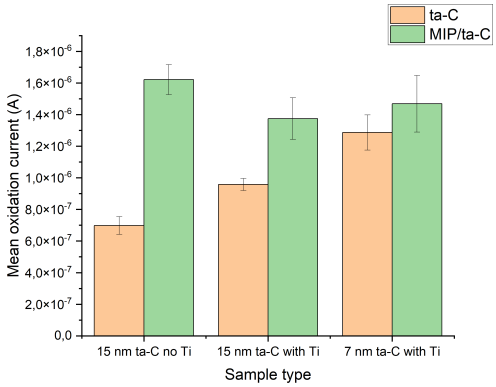

Figure 4.30: Column plot of the mean oxidation currents for different samples under analysis

shown in both figures 4.30 and 4.31. This is due to the fact that thinner ta-C have a higher fraction of sp^2, as they make the sample more graphite-like, improving its conductivity. On the opposite, sp^3 orbitals make the film diamond-like and therefore less conductive. As a consequence, the resistance is reduced for lower thickness. This ensures a better electron transfer through the layer and to the copper substrate [44, 52, 45].

Considering instead the effect of the titanium coating, it can be seen that the titanium improves the performance of the electrode, as shown in figure 4.30 and 4.32. This can be attributed to the better conductivity of the titanium compared to ta-C, which provides an easier path for the electron transport and a better electrical contact [45].

From the figures presented it is clear that the best sample among the ones analysed for unmodified ta-C can be considered to be the 7 nm ta-C sample with the titanium adhesion layer.

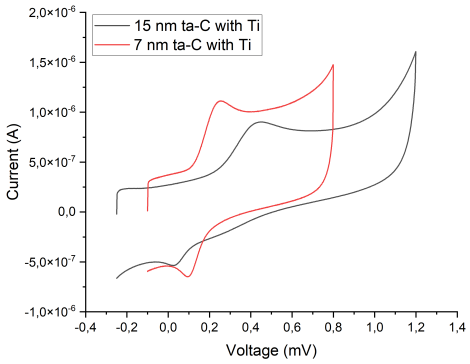

Figure 4.31: Comparison of the CV studies for 7 nm ta-C with titanium adhesion layer and 15 nm ta-C with titanium adhesion layer to assess the effect of the ta-C thickness

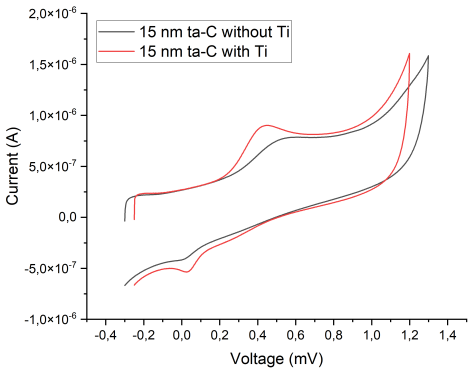

Figure 4.32: Comparison of the CV studies for 15 nm ta-C with titanium adhesion layer and 15 nm ta-C without titanium adhesion layer to assess the effect of the presence of the titanium adhesion layer

Let us now consider the MIP/ta-C modified samples. It is important to point out that the potential window in the CV studies was varied according to the sample and the position of the oxidation and reduction peaks. The CV curves for the MIP/ta-C modified samples are shown in figures 4.33 and 4.34.

From figure 4.33 it is clear that a lower thickness of the ta-C layer improves the performance of the electrode. As mentioned above, this can be related to an easier electron transfer through the ta-C layer.

Considering figure 4.34, it can be said that the effect of titanium worsens the electrode performance. The effect of the titanium layer is the opposite of that found for the unmodified ta-C. This can be attributed to the presence of the PPy, which is altering the structure of the sample and the electron transport.

The best material among the ones analyzed has been found to be the one with the 15 nm ta-C layer without titanium adhesion layer for the MIP/ta-C samples.

However, the sample with the 7 nm ta-C coating is practically within error margins both with or without MIP modification. The changes provided by the presence of the titanium adhesion layer and by the presence of MIP modification are strongly enhanced for the 15 nm ta-C samples. This implies that the stronger

improvements are achieved for a thicker sample.

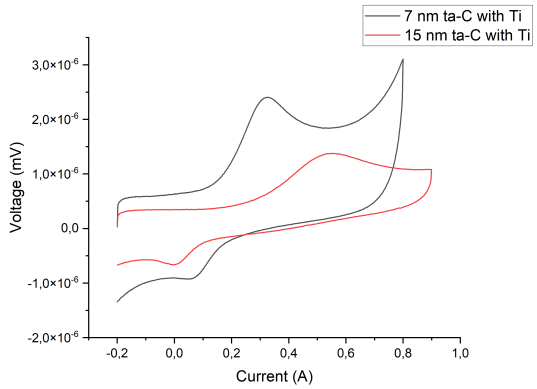

Figure 4.33: Comparison of the CV studies for 7 nm ta-C with titanium adhesion layer and 15 nm with titanium adhesion layer MIP/ta-C samples to assess the effect of the ta-C thickness

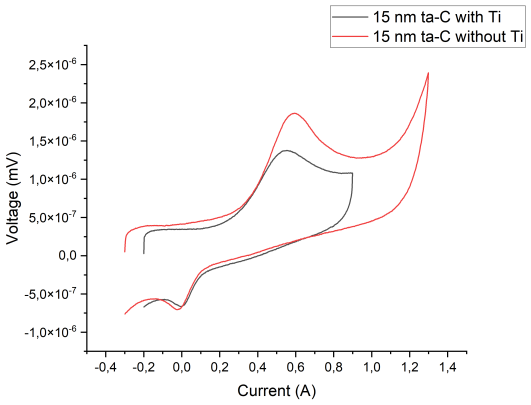

Figure 4.34: Comparison of the CV studies for 15 nm ta-C with titanium adhesion layer and 15 nm without titanium adhesion layer MIP/ta-C samples to assess the effect of the presence of the titanium adhesion layer

4.7 Effect of the presence of interferents in the solution

The effect of the presence of interferents has been taken into account by considering the performance of the electrodes in a solution of DA and AA.

The same study has been carried out by Palomäki et al. for plain ta-C and it is reported in this work [52]. Considering figure 4.35 it is clear that ta-C is not selective towards DA, as the signal for AA shades the DA signal even in large concentrations like that considered in this study.

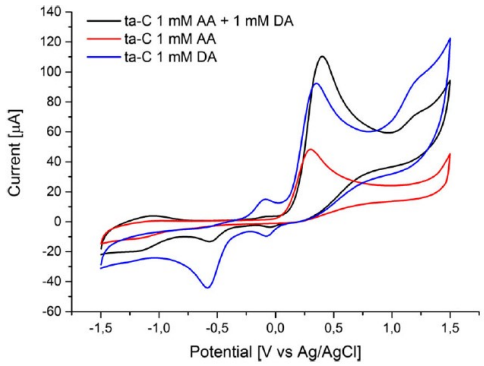

Figure 4.35: CV studies in the presence of AA and DA in different concentrations for plain ta-C [52]

The same study has been repeated for MIP/ta-C electrodes and figure 4.36 shows the results. The physiological concentration of AA and DA has been first considered:

- DA: 10 μM
- AA: 1 mM

In this case the DA signal is shaded by the AA one. As a result, it can be stated that the sensor is not selective towards DA. The signal for the 10 μM DA solution is at a similar potential to that of AA and it is clearly too low to show. When the concentration of DA is increased to 1 mM the reduction peak becomes visible, leading to an easier detection of the analyte.

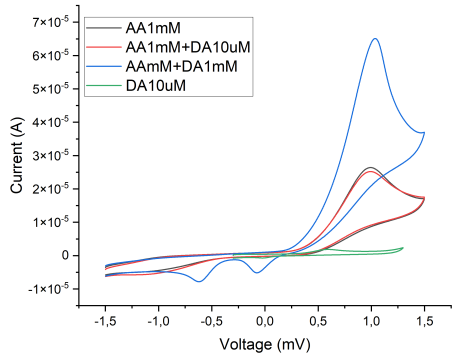

Figure 4.36: CV studies in the presence of AA and DA in different concentrations for MIP/ta-C electrodes

The same study was carried out for different samples, including the presence of carbon nanofibers (CNFs) and carbon nanotubes (CNTs) on the ta-C surface. Such electrodes provided instead a high selectivity towards their target analyte, showing an improvement when compared to the present case [34, 51].

The physiological concentration of AA is several orders of magnitude higher than the concentration of DA. This is the reason why the DA signal is easily shaded, unless the sensor is highly selective. However, it has been shown that AA decays rapidly in cell culture media and it is no longer detected by the sensor after an incubation time, whilst NTs can still be observed. Rantataro et al. have shown that AA has a half-time of 2.1 hours and its concentration is decreased by 93% after 8 hours and by 99.75% after an 18-hour incubation time. As a consequence, the lack of selectivity might not affect the performance of the developed electrodes in cell culture media, the target medium of this study [53]. However, the selectivity can still be considered to be a problem when considering physiological fluids (plasma, serum or urine for example).

4.8 Reproducibility, repeatability

The reproducibility and repeatability have been considered during the different studies and some considerations are discussed in this section.

The reproducibility has been qualitatively measured considering the behaviour of different electrodes in the same conditions. Several electrodes (3-5) were always used for a measurement in the same conditions, in order to be able to understand their behaviour. The standard deviation in the response signal was mostly found to be low, leading to the conclusion that the reproducibility of the process is good. As a result, different electrodes are able to provide similar results when tested in the same conditions.

As a proof, 10 different electrodes used during the studies were compared in order to assess quantitatively the reproducibility of the studies. Figure 4.37 gives an idea about the reproducibility of the studies carried out during this work, proving that the electrodes provide similar results when used in the same experimental conditions. The standard deviation of the current for the 10 electrodes shown in figure 4.37 has been computed and found to be $1.18 \cdot 10^{-7}\, A$, which is an acceptable result.

Repeatability was instead qualitatively measured considering the behaviour of the same electrode in the same conditions for several times. More specifically, the same electrode was used for DA detection a first time and then washed by CV in order to remove the DA target molecules stuck in the recognition sites. The electrode was then used again in the same conditions. Unfortunately, the performance of the electrode has been found to decrease for multiple uses, as the

response signal was decreased after the first used. The number of active recognition sites seems to be decreased after the washing process of the used electrode, leading to a decrease in its signal when compared to the performance of a fresh electrode. This implies that the process is not repeatable and that each electrode should be used only once. For this reason, all the studies carried out in this work were performed using fresh electrodes.

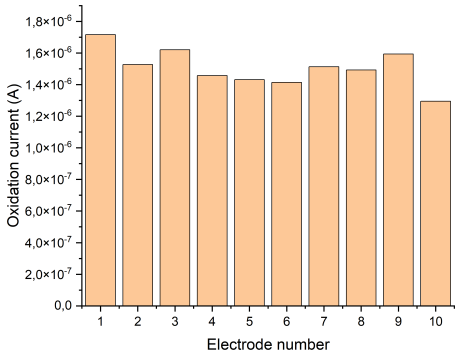

Figure 4.37: Oxidation current for different electrodes used in the same experimental conditions

Conclusion

As mentioned in the previous chapters, the present work was meant to develop an ultra-sensitive MIP-based electrochemical sensor for the detection of DA. The sensor obtained is compatible with common microsystem technologies, miniaturizable and it can be integrated on a chip. As a consequence in the future it will be able to provide real time monitoring when integrated in a system-on-chip device.

At the the beginning of the work, the experimental conditions for the molecular imprinting have been optimized in order to ensure the best results possible. The electropolymerization of the PPy on top of the ta-C has been proved during various experiments, both electrochemical studies and physical characterization. The coupling of MIPs and carbon nanomaterials has allowed to obtain a combination of the benefits of them both, improving the performance of the sensor and allowing to reach most of the preset goals.

Sensitivity was strongly improved if compared to the bare ta-C studies carried out previously, bringing it down to $162\,nM$ with an LOD of $48.6\,nM$ in the dynamic linear range between $100\,nM$ and $1\,\mu M$. This is a physiological relevant sensitivity, which makes the sensor valuable for *in vitro* studies.

Electrochemical studies have proved the higher performance of MIP/ta-C electrode compared to unmodified ta-C ones. This implies that the methodology used is effective for the ultra-sensitive detection of DA for carbon-based sensing systems.

In addition, it is important to point out that most of the works analysed in section 1.6 (state of the art) consider optimized pH for the detection. The sensor developed in this study works in physiological pH, making it even more suitable for *in vitro* experiments.

Last, the sensor developed is fully biocompatible as proved in other studies such as [52]. This implies that, in principle, the sensor could be used to grow cell cultures.

Unfortunately, the selectivity of the present electrodes was as poor as for plain ta-C. This problem is solved when carbon nanofibers or carbon nanotubes are grown on the ta-C substrate, providing a larger surface area and a better selectivity towards DA, as discussed in [5] and [52]. The lack of selectivity is related to overlapping of the redox peaks in the CV scans, leading to the shadowing of the

DA signal. This can be overcome by shifting the oxidation potential by means of defects, metal nanoparticles or the presence of edge plains, for example [5]. The lack of selectivity can considered to be overcome when working in cell culture media, although it is still a problem in physiological fluids [53].

Appendix A

Appendix 1: Electrical double leyer (EDL)

In order for the interface between the electrode and the solution to remain neutral and to compensate for the excess charge on the electrode, an *electrical double layer* (EDL) is formed, as shown in figure A.1.

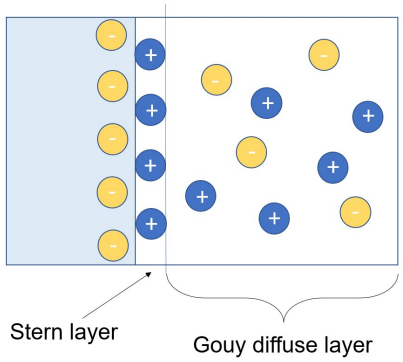

Figure A.1: Schematic figure of the EDL

The ELD is defined as an array of charged particles and oriented dipoles at every material interface and, in particular, at the electrode interface. Its goal is to keep the interface neutral, balancing the charge held on the electrode redistributing the ions close to the electrode's surface [20]. The electrical double layer will be positively charged for negatively charged electrodes and vice versa for positively charged electrodes, as the interface should be neutral [20]. The charge on the electrode (q_e) and the one due to the ions in the nearby solution (q_s) should therefore balance [20]:

$$q_e + q_s = 0 \tag{A.1}$$

The inner layer of the electrical double layer is identified as *inner Helmholtz plane* (IHP) and it is made of solvent molecules and specifically adsorbed ions. Moving away from the electrode, the *outer Helmholtz plane* (OHP) is found, which is the imaginary plane passing through the center of the solvated ions closest to the surface: they are non-specifically adsorbed and they are attracted to the surface by a long-range coulomb force. The IHP and the OHP together make the compact layer, also called Stern layer, strongly held by the electrode. It is important to point out that this model does not take into account the thermal motion of ions [20]. The outer layer is called *diffuse layer* or *Gouy layer* and it extends from the OHP into the bulk solution [20]. Two forces are counteracting in this scenario: the ordering electrical field and random thermal motion. These two effects must balance, leading to an exponential decrease of the concentration of ionic species at a given distance from the surface. In particular:

$$C(x) = C(0)exp(\frac{-zF\phi}{RT}) \tag{A.2}$$

where the numerator of the exponential function represents the electrostatic energy and the denominator stands for the thermal one. The charge belonging to both the diffuse layer and compact one balances the one on the electrode. Figure A.1 shows the distribution of the potential with respect to the distance from the electrode: it includes a linear region close to the electrode and an exponential one from the OHP on.

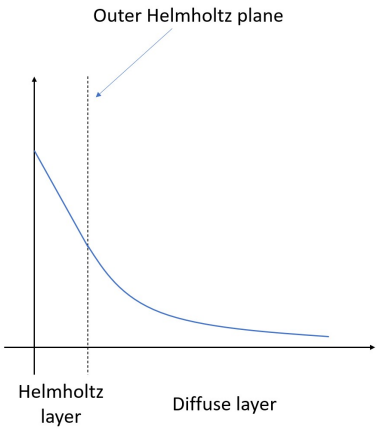

Figure A.2: Electrical double layer potential profile

The electrical double layer behaves like a parallel plate capacitor which capacitance is described by the series of the capacitances of the diffuse layer (Gouy layer) and the compact layer (Helmholtz layer):

$$\frac{1}{C} = \frac{1}{C_H} + \frac{1}{C_G} \tag{A.3}$$

The capacitance related to the Gouy layer (C_G) is strongly related to the concentration of the electrolyte. [20].

Bibliography

[1] Tomi Laurila, Vera Protopopova, Sneha Rhode, Sami Sainio, Tommi Palomäki, Michelle Moram, Juan M. Feliu, and Jari Koskinen. «New electrochemically improved tetrahedral amorphous carbon films for biological applications». In: *Diamond and Related Materials* 49 (2014), pp. 62–71. ISSN: 0925-9635. DOI: https://doi.org/10.1016/j.diamond.2014.08.007. URL: https://www.sciencedirect.com/science/article/pii/S0925963514001654 (cit. on pp. 1, 29, 30).

[2] Bo Si and Edward Song. «Recent Advances in the Detection of Neurotransmitters». In: *Chemosensors* 6.1 (2018). ISSN: 2227-9040. URL: https://www.mdpi.com/2227-9040/6/1/1 (cit. on pp. 1, 2, 7, 17).

[3] Zahra Tavakolian-Ardakani, Oana Hosu, Cecilia Cristea, Mohammad Mazloum-Ardakani, and Giovanna Marrazza. «Latest Trends in Electrochemical Sensors for Neurotransmitters: A Review». In: *Sensors* 19.9 (2019). ISSN: 1424-8220. DOI: 10.3390/s19092037. URL: https://www.mdpi.com/1424-8220/19/9/2037 (cit. on pp. 1, 2, 6, 7, 10, 11, 17).

[4] Günther Deuschl, Ettore Beghi, Franz Fazekas, Timea Varga, Kalliopi A. Christoforidi, Eveline Sipido, Claudio L. Bassetti, Theo Vos, and Valery L. Feigin. «The burden of neurological diseases in Europe: an analysis for the Global Burden of Disease Study 2017». In: *The Lancet Public Health* 5.10 (2020). doi: 10.1016/S2468-2667(20)30190-0, e551–e567. ISSN: 2468-2667. DOI: 10.1016/S2468-2667(20)30190-0. URL: https://doi.org/10.1016/S2468-2667(20)30190-0 (cit. on p. 1).

[5] Tomi Laurila, Sami Sainio, and Miguel A. Caro. «Hybrid carbon based nanomaterials for electrochemical detection of biomolecules». In: *Progress in Materials Science* 88 (2017), pp. 499–594. ISSN: 0079-6425. DOI: https://doi.org/10.1016/j.pmatsci.2017.04.012. URL: https://www.sciencedirect.com/science/article/pii/S0079642517300518 (cit. on pp. 1, 28–32, 77, 78).

[6] Nidhi Chauhan, Shringika Soni, Prabhudatt Agrawal, Yatan Pal Singh Balhara, and Utkarsh Jain. «Recent advancement in nanosensors for neurotransmitters detection: Present and future perspective». In: *Process Biochemistry* 91 (2020), pp. 241–259. ISSN: 1359-5113. DOI: https://doi.org/10.1016/j.procbio.2019.12.016. URL: https://www.sciencedirect.com/science/article/pii/S1359511319314035 (cit. on pp. 1, 5–7, 10, 11, 17, 33).

[7] Xixia Liu and Juewen Liu. «Biosensors and sensors for dopamine detection». In: *VIEW* 2.1 (2021), p. 20200102. DOI: https://doi.org/10.1002/VIW.20200102. eprint: https://onlinelibrary.wiley.com/doi/pdf/10.1002/VIW.20200102. URL: https://onlinelibrary.wiley.com/doi/abs/10.1002/VIW.20200102 (cit. on pp. 2, 6, 8, 9, 17, 22, 24, 27, 28, 31, 33).

[8] K. Santoro and C. Ricciardi. «Biosensors». In: *Encyclopedia of Food and Health*. Ed. by Benjamin Caballero, Paul M. Finglas, and Fidel Toldrá. Oxford: Academic Press, 2016, pp. 430–436. ISBN: 978-0-12-384953-3. DOI: https://doi.org/10.1016/B978-0-12-384947-2.00072-6. URL: https://www.sciencedirect.com/science/article/pii/B9780123849472000726 (cit. on pp. 2, 12–14).

[9] Z. L. Kruk and C. Pycock. *Neurotransmitters and Drugs*. Ed. by Springer Netherlands. Third. n.d.: Springer-Verlag, 1991 (cit. on pp. 4, 5, 7).

[10] Jianshi Tang et al. «Bridging Biological and Artificial Neural Networks with Emerging Neuromorphic Devices: Fundamentals, Progress, and Challenges». In: *Advanced Materials* 31.49 (2019), p. 1902761. DOI: https://doi.org/10.1002/adma.201902761. eprint: https://onlinelibrary.wiley.com/doi/pdf/10.1002/adma.201902761. URL: https://onlinelibrary.wiley.com/doi/abs/10.1002/adma.201902761 (cit. on pp. 4–6).

[11] Queensland Brain Institute. *What are neurotransmitters?* Web Page. URL: https://qbi.uq.edu.au/brain/brain-physiology/what-are-neurotransmitters#:~:text=Neurotransmitters%20are%20often%20referred%20to,or%20from%20neurons%20to%20muscles.&text=Most%20neurotransmitters%20are%20either%20small,%2C%20amino%20acids%2C%20or%20neuropeptides (cit. on p. 5).

[12] Saikat Banerjee, Stephanie McCracken, Md Faruk Hossain, and Gymama Slaughter. «Electrochemical Detection of Neurotransmitters». In: *Biosensors* 10.8 (2020). ISSN: 2079-6374. DOI: 10.3390/bios10080101. URL: https://www.mdpi.com/2079-6374/10/8/101 (cit. on pp. 6, 8, 9, 14, 15, 17, 21, 31, 35).

[13] The Nobel Prize. *Otto Loewi, biographical*. Web Page. URL: https://www.nobelprize.org/prizes/medicine/1936/loewi/biographical/ (cit. on p. 7).

[14] Nihal Ermiş and Nihat Tinkiliç. «Development of an Electrochemical Sensor for Selective Determination of Dopamine Based on Molecularly Imprinted Poly(p-aminothiophenol) Polymeric Film». In: *Electroanalysis* 33.6 (2021), pp. 1491–1501. DOI: https://doi.org/10.1002/elan.202060556. URL: https://analyticalsciencejournals.onlinelibrary.wiley.com/doi/abs/10.1002/elan.202060556 (cit. on pp. 7, 9, 23, 25, 34, 36, 37).

[15] Saheed E. Elugoke, Abolanle S. Adekunle, Omolola E. Fayemi, Ekemini D. Akpan, Bhekie B. Mamba, El-Sayed M. Sherif, and Eno E. Ebenso. «Molecularly imprinted polymers (MIPs) based electrochemical sensors for the determination of catecholamine neurotransmitters – Review». In: *Electrochemical Science Advances* 1.2 (2021), e2000026. DOI: https://doi.org/10.1002/elsa.202000026. eprint: https://chemistry-europe.onlinelibrary.wiley.com/doi/pdf/10.1002/elsa.202000026. URL: https://chemistry-europe.onlinelibrary.wiley.com/doi/abs/10.1002/elsa.202000026 (cit. on pp. 7, 12, 23, 24, 26, 27, 33).

[16] S. Colette Daubner, Tiffany Le, and Shanzhi Wang. «Tyrosine hydroxylase and regulation of dopamine synthesis». In: *Archives of Biochemistry and Biophysics* 508.1 (2011), pp. 1–12. ISSN: 0003-9861. DOI: 10.1016/j.abb.2010.12.017. URL: https://dx.doi.org/10.1016/j.abb.2010.12.017 (cit. on pp. 7, 8).

[17] Tommi Palomäki, Sara Chumillas, Sami Sainio, Vera Protopopova, Minna Kauppila, Jari Koskinen, Víctor Climent, Juan M. Feliu, and Tomi Laurila. «Electrochemical reactions of catechol, methylcatechol and dopamine at tetrahedral amorphous carbon (ta-C) thin film electrodes». In: *Diamond and Related Materials* 59 (2015), pp. 30–39. ISSN: 0925-9635. DOI: https://doi.org/10.1016/j.diamond.2015.09.003. URL: https://www.sciencedirect.com/science/article/pii/S0925963515300340 (cit. on pp. 9, 17, 31).

[18] Shabi Abbas Zaidi. «Development of molecular imprinted polymers based strategies for the determination of Dopamine». In: *Sensors and Actuators B: Chemical* 265 (2018), pp. 488–497. ISSN: 0925-4005. DOI: https://doi.org/10.1016/j.snb.2018.03.076. URL: https://www.sciencedirect.com/science/article/pii/S0925400518305665 (cit. on pp. 9, 12, 22–24, 26, 27, 32).

[19] Aoife C. Power and Aoife Morrin. «Electroanalytical Sensor Technology». In: *Electrochemistry*. Ed. by Mohammed A. A. Khalid. Rijeka: IntechOpen, 2013. Chap. 7. DOI: 10.5772/51480. URL: https://doi.org/10.5772/51480 (cit. on pp. 10–14, 16, 17, 23, 31).

[20] Joseph Wang. *Analytical Electrochemistry*. Second. John Wiley Sons, INC., 2000. ISBN: 0471-28272-3 (cit. on pp. 12, 13, 15, 16, 79–81).

[21] Elli Leppänen, Anja Aarva, Sami Sainio, Miguel A Caro, and Tomi Laurila. «Connection between the physicochemical characteristics of amorphous carbon thin films and their electrochemical properties». In: *Journal of Physics: Condensed Matter* 33.43 (Aug. 2021), p. 434002. DOI: 10.1088/1361-648x/ac1a2e. URL: https://doi.org/10.1088/1361-648x/ac1a2e (cit. on pp. 17, 26, 29, 30).

[22] Kourosh Kalantar-zadeh. *Sensors: An Introductory Course*. 1st ed. Springer New York, NY, 2013. ISBN: 978-1-4614-5052-8. DOI: https://doi.org/10.1007/978-1-4614-5052-8 (cit. on p. 18).

[23] Thanh-Hai Le, Yukyung Kim, and Hyeonseok Yoon. «Electrical and Electrochemical Properties of Conducting Polymers». In: *Polymers* 9.4 (2017). ISSN: 2073-4360. DOI: 10.3390/polym9040150. URL: https://www.mdpi.com/2073-4360/9/4/150 (cit. on pp. 19–21, 32).

[24] Namsheer K and Chandra Sekhar Rout. «Conducting polymers: a comprehensive review on recent advances in synthesis, properties and applications». In: *RSC Adv.* 11 (10 2021), pp. 5659–5697. DOI: 10.1039/D0RA07800J. URL: http://dx.doi.org/10.1039/D0RA07800J (cit. on pp. 19–22).

[25] Lin Xia, Zhixiang Wei, and Meixiang Wan. «Conducting polymer nanostructures and their application in biosensors». In: *Journal of Colloid and Interface Science* 341.1 (2010), pp. 1–11. ISSN: 0021-9797. DOI: https://doi.org/10.1016/j.jcis.2009.09.029. URL: https://www.sciencedirect.com/science/article/pii/S0021979709012120 (cit. on pp. 20, 21).

[26] C.I. Awuzie. «Conducting Polymers». In: *Materials Today: Proceedings* 4.4, Part E (2017). International Conference on Multifunctional Materials for Device Applications (ICMDA-2016), October 26-28, 2016, pp. 5721–5726. ISSN: 2214-7853. DOI: https://doi.org/10.1016/j.matpr.2017.06.036. URL: https://www.sciencedirect.com/science/article/pii/S2214785317308088 (cit. on pp. 21, 22).

[27] Nihal Ermis. «Preparation of Molecularly Imprınted Polypyrrole Modified Gold Electrode for Determination of Tyrosine in Biological Samples». In: *International Journal of Electrochemical Science* 13 (Mar. 2018), pp. 2286–2298. DOI: 10.20964/2018.03.29 (cit. on pp. 22, 25, 26).

[28] Qun Cao, Pumidech Puthongkham, and B. Jill Venton. «Review: new insights into optimizing chemical and 3D surface structures of carbon electrodes for neurotransmitter detection». In: *Anal. Methods* 11 (3 2019), pp. 247–261. DOI: 10.1039/C8AY02472C. URL: http://dx.doi.org/10.1039/C8AY02472C (cit. on pp. 22, 28, 29, 31, 32).

[29] Yeşeren Saylan, Fatma Yilmaz, Erdoğan Özgür, Ali Derazshamshir, Handan Yavuz, and Adil Denizli. «Molecular Imprinting of Macromolecules for Sensor Applications». In: *Sensors* 17.4 (2017). ISSN: 1424-8220. DOI: 10.3390/s17040898. URL: https://www.mdpi.com/1424-8220/17/4/898 (cit. on pp. 24, 27).

[30] Sami Sainio. «Carbon based hybrid nanomaterials for electrochemical detection of neurotransmitters». English. Doctoral thesis. School of Electrical Engineering, 2017, 71 + app. 57. ISBN: 978-952-60-7389-7 (electronic), 978-952-60-7390-3 (printed). URL: http://urn.fi/URN:ISBN:978-952-60-7389-7 (cit. on p. 28).

[31] Debabrata Maiti, Xiangmin Tong, Xiaozhou Mou, and Kai Yang. «Carbon-Based Nanomaterials for Biomedical Applications: A Recent Study». In: *Frontiers in Pharmacology* 9 (2019). ISSN: 1663-9812. DOI: 10.3389/fphar.2018.01401. URL: https://www.frontiersin.org/article/10.3389/fphar.2018.01401 (cit. on p. 28).

[32] Khadijeh Nekoueian. «Modification of carbon-based electrodes using metal nanostructures: application to voltammetric determination of some pharmaceutical and biological compounds». Thesis. 2019 (cit. on pp. 28, 31).

[33] S. E. Rodil, R. Olivares, and H. Arzate. «In vitro cytotoxicity of amorphous carbon films». In: *Bio-Medical Materials and Engineering* 15 (2005), pp. 101–112 (cit. on pp. 29, 30).

[34] S. Sainio, T. Palomäki, N. Tujunen, V. Protopopova, J. Koehne, K. Kordas, J. Koskinen, M. Meyyappan, and T. Laurila. «Integrated Carbon Nanostructures for Detection of Neurotransmitters». In: *Mol Neurobiol* 52.2 (2015). 1559-1182 Sainio, Sami Palomäki, Tommi Tujunen, Noora Protopopova, Vera Koehne, Jessica Kordas, Krisztian Koskinen, Jari Meyyappan, M Laurila, Tomi Evaluation Study Journal Article United States 2015/06/22 Mol Neurobiol. 2015 Oct;52(2):859-66. doi: 10.1007/s12035-015-9233-z., pp. 859–66. ISSN: 0893-7648. DOI: 10.1007/s12035-015-9233-z (cit. on pp. 29, 75).

[35] Emilia Peltola, Anja Aarva, Sami Sainio, Joonas J. Heikkinen, Niklas Wester, Ville Jokinen, Jari Koskinen, and Tomi Laurila. «Biofouling affects the redox kinetics of outer and inner sphere probes on carbon surfaces drastically differently – implications to biosensing». In: *Phys. Chem. Chem. Phys.* 22 (29 2020), pp. 16630–16640. DOI: 10.1039/D0CP02251A. URL: http://dx.doi.org/10.1039/D0CP02251A (cit. on p. 30).

[36] T. Goto, T. Yasukawa, K. Kanda, S. Matsui, and F. Mizutani. «Inhibition of electrochemical fouling against biomolecules on a diamond-like carbon electrode». In: *Anal Sci* 27.1 (2011). 1348-2246 Goto, Takuya Yasukawa,

Tomoyuki Kanda, Kazuhiro Matsui, Shinji Mizutani, Fumio Journal Article Research Support, Non-U.S. Gov't Switzerland 2011/01/15 Anal Sci. 2011;27(1):91-4. doi: 10.2116/analsci.27.91., pp. 91–4. ISSN: 0910-6340. DOI: 10.2116/analsci.27.91 (cit. on p. 30).

[37] Zhiwei Lu et al. «A dual-template imprinted polymer electrochemical sensor based on AuNPs and nitrogen-doped graphene oxide quantum dots coated on NiS2/biomass carbon for simultaneous determination of dopamine and chlorpromazine». In: *Chemical Engineering Journal* 389 (2020), p. 124417. ISSN: 1385-8947. DOI: https://doi.org/10.1016/j.cej.2020.124417. URL: https://www.sciencedirect.com/science/article/pii/S1385894720304083 (cit. on pp. 33, 36, 37).

[38] Vinu Mohan Allibai Mohanan, Aswini Kacheri Kunnummal, and Valsala Madhavan Nair Biju. «Selective electrochemical detection of dopamine based on molecularly imprinted poly(5-amino 8-hydroxy quinoline) immobilized reduced graphene oxide». In: *Journal of Materials Science* 53.15 (2018), pp. 10627–10639. ISSN: 1573-4803. DOI: 10.1007/s10853-018-2355-8. URL: https://doi.org/10.1007/s10853-018-2355-8 (cit. on pp. 34, 36, 37).

[39] Yonghai Song, Jiajia Han, Lijuan Xu, Longfei Miao, Canwei Peng, and Li Wang. «A dopamine-imprinted chitosan Film/Porous ZnO NPs@carbon Nanospheres/Macroporous carbon for electrochemical sensing dopamine». In: *Sensors and Actuators B: Chemical* 298 (2019), p. 126949. ISSN: 0925-4005. DOI: https://doi.org/10.1016/j.snb.2019.126949. URL: https://www.sciencedirect.com/science/article/pii/S0925400519311487 (cit. on pp. 34, 36, 37).

[40] Bo Si and Edward Song. «Molecularly imprinted polymers for the selective detection of multi-analyte neurotransmitters». In: *Microelectronic Engineering* 187-188 (2018), pp. 58–65. ISSN: 0167-9317. DOI: https://doi.org/10.1016/j.mee.2017.11.016. URL: https://www.sciencedirect.com/science/article/pii/S0167931717303921 (cit. on pp. 34, 36, 37).

[41] Taira Kajisa, Wei Li, Tsuyoshi Michinobu, and Toshiya Sakata. «Well-designed dopamine-imprinted polymer interface for selective and quantitative dopamine detection among catecholamines using a potentiometric biosensor». In: *Biosensors and Bioelectronics* 117 (2018), pp. 810–817. ISSN: 0956-5663. DOI: https://doi.org/10.1016/j.bios.2018.07.014. URL: https://www.sciencedirect.com/science/article/pii/S0956566318305141 (cit. on pp. 34, 36, 37).

[42] Xue Ma, Feng Gao, Runying Dai, Guangbin Liu, Ying Zhang, Limin Lu, and Yongfang Yu. «Novel electrochemical sensing platform based on a molecularly imprinted polymer-decorated 3D-multi-walled carbon nanotube intercalated

graphene aerogel for selective and sensitive detection of dopamine». In: *Anal. Methods* 12 (14 2020), pp. 1845–1851. DOI: 10.1039/D0AY00033G. URL: http://dx.doi.org/10.1039/D0AY00033G (cit. on pp. 35–37).

[43] Jiao Yang, Yue Hu, and Yingchun Li. «Molecularly imprinted polymer-decorated signal on-off ratiometric electrochemical sensor for selective and robust dopamine detection». In: *Biosensors and Bioelectronics* 135 (2019), pp. 224–230. ISSN: 0956-5663. DOI: https://doi.org/10.1016/j.bios.2019.03.054. URL: https://www.sciencedirect.com/science/article/pii/S0956566319302702 (cit. on pp. 35–37).

[44] Tommi Palomäki, Emilia Peltola, Sami Sainio, Niklas Wester, Olli Pitkänen, Krisztian Kordas, Jari Koskinen, and Tomi Laurila. «Corrigendum to "Unmodified and multi-walled carbon nanotube modified tetrahedral amorphous carbon (ta-C) films as in vivo sensor materials for sensitive and selective detection of dopamine" [Bios. Bioelectron. 118 (2018) 23–30]». In: *Biosensors and Bioelectronics* 123 (2019), pp. 281–284. ISSN: 0956-5663. DOI: 10.1016/j.bios.2018.08.053. URL: https://dx.doi.org/10.1016/j.bios.2018.08.053 (cit. on pp. 55, 58, 61, 63, 71).

[45] Tommi Palomäki, Niklas Wester, Miguel A. Caro, Sami Sainio, Vera Protopopova, Jari Koskinen, and Tomi Laurila. «Electron transport determines the electrochemical properties of tetrahedral amorphous carbon (ta-C) thin films». In: *Electrochimica Acta* 225 (2017), pp. 1–10. ISSN: 0013-4686. DOI: https://doi.org/10.1016/j.electacta.2016.12.099. URL: https://www.sciencedirect.com/science/article/pii/S0013468616326585 (cit. on pp. 58, 62, 63, 71).

[46] Jarkko Etula et al. «What Determines the Electrochemical Properties of Nitrogenated Amorphous Carbon Thin Films?» In: *Chemistry of Materials* 33.17 (2021), pp. 6813–6824. DOI: 10.1021/acs.chemmater.1c01519. eprint: https://doi.org/10.1021/acs.chemmater.1c01519. URL: https://doi.org/10.1021/acs.chemmater.1c01519 (cit. on p. 61).

[47] Andrzej Lasia. *A. Lasia, Electrochemical Impedance Spectroscopy and its Applications, book, Springer, 2014*. July 2014. ISBN: 978-1-4614-8932-0. DOI: 10.1007/978-1-4614-8933-7 (cit. on p. 62).

[48] Reza Ansari. «Polypyrrole Conducting Electroactive Polymers: Synthesis and Stability Studies». In: *Journal of Chemistry* 3 (Nov. 2006), pp. 186–201. DOI: 10.1155/2006/860413 (cit. on p. 63).

[49] Noémie Elgrishi, Kelley J. Rountree, Brian D. McCarthy, Eric S. Rountree, Thomas T. Eisenhart, and Jillian L. Dempsey. «A Practical Beginner's Guide to Cyclic Voltammetry». In: *Journal of Chemical Education* 95.2 (2018). doi: 10.1021/acs.jchemed.7b00361, pp. 197–206. ISSN: 0021-9584. DOI:

10.1021/acs.jchemed.7b00361. URL: https://doi.org/10.1021/acs.jchemed.7b00361 (cit. on pp. 66, 67).

[50] Yingchun Li et al. «Novel Electrochemical Sensing Platform Based on a Molecularly Imprinted Polymer Decorated 3D Nanoporous Nickel Skeleton for Ultrasensitive and Selective Determination of Metronidazole». In: *ACS Applied Materials Interfaces* 7.28 (2015). doi: 10.1021/acsami.5b03755, pp. 15474–15480. ISSN: 1944-8244. DOI: 10.1021/acsami.5b03755. URL: https://doi.org/10.1021/acsami.5b03755 (cit. on p. 68).

[51] Sami Sainio et al. «Integrating Carbon Nanomaterials with Metals for Biosensing Applications». In: *Molecular Neurobiology* 57.1 (2020), pp. 179–190. ISSN: 1559-1182. DOI: 10.1007/s12035-019-01767-7. URL: https://doi.org/10.1007/s12035-019-01767-7 (cit. on pp. 70, 75).

[52] Tommi Palomäki, Emilia Peltola, Sami Sainio, Niklas Wester, Olli Pitkänen, Krisztian Kordas, Jari Koskinen, and Tomi Laurila. «Unmodified and multiwalled carbon nanotube modified tetrahedral amorphous carbon (ta-C) films as in vivo sensor materials for sensitive and selective detection of dopamine». In: *Biosensors and Bioelectronics* 118 (2018), pp. 23–30. ISSN: 0956-5663. DOI: https://doi.org/10.1016/j.bios.2018.07.018. URL: https://www.sciencedirect.com/science/article/pii/S0956566318305190 (cit. on pp. 71, 73, 74, 77).

[53] Tomi Laurila Samuel Rantataro Laura Ferrer Pascual. «Ascorbic acid does not necessarily interfere with the electrochemical detection of neurotransmitters». In: *Biosensors and Bioelectronics* (2022). DOI: https://dx.doi.org/10.2139/ssrn.4111370. URL: https://papers.ssrn.com/sol3/papers.cfm?abstract_id=4111370 (cit. on pp. 75, 78).